Computer Assisted Mechanics and Engineering Sciences, **13**: 53–83, 2006.

Shaping the stiffest three-dimensional structures from two given isotropic materials

Sławomir Czarnecki, Tomasz Lewiński
Faculty of Civil Engineering, Warsaw University of Technology,
Al. Armii Ludowej 16, 00-637 Warsaw, Poland

(Received in the final form February 15, 2006)

The paper concerns layout optimization of elastic three dimensional bodies composed of two isotropic materials of given amount. Optimal distribution of the materials corresponds to minimization of the total compliance or the work of the given design-independent loading. The problem is discussed in its relaxed form admitting composite domains, according to the known theoretical results on making the minimum compliance problems well posed. The approach is based upon explicit formulae for the components of Hooke's tensor of the third rank stiff two material composites. An appropriate derivation of these formulae is provided. The numerical algorithm is based on COC concept, the equilibrium problems being solved by the ABAQUS system. Some of the optimal layouts presented compare favourably with the known benchmark solutions. The paper shows how to use commercial FEM codes to find optimal composite designs within linear elasticity theory.

1. Introduction

Two isotropic materials suffice to form a composite of extremal anisotropic properties of given volume fractions. This surprising result is due to Milton and Cherkaev [33], see Milton [32], Cherkaev [9]. Moreover, two isotropic materials of bulk: κ_2, κ_1 and shear: μ_2, μ_1, ordered moduli such that $\kappa_2 > \kappa_1$, $\mu_2 > \mu_1$, can serve for construction of the bodies of minimal compliance. This construction is abstract. It consists in consecutive stacking of the stiffer (or stronger) constituent with the weaker one and then stacking the stiffer constituent with the mixtures obtained in the previous stages, in three mutually orthogonal directions. Such a composite is called stiff since the stiffer component is used three times, while the weaker one is present only at the first stage of stacking. This composite is also called hierarchical since the length scales of the laminations are of descending order. It turns out that this sub-class of two-component composites is sufficient to attain minimum of the total compliance of the three dimensional elastic bodies, see Theorem 4.1.12 in Allaire [2]. This theorem says that the relaxation by homogenization of the minimum compliance problem is correct and can be constructed with using the mentioned class of composites.

The two-dimensional counterpart of this theorem says that the minimum compliance of plates loaded in plane (so called 2D elasticity problem) composed of two isotropic materials is attained within the class of orthotropic plates made of the 2nd rank stiff laminates; this theorem has been proposed by Gibiansky and Cherkaev [22], see Allaire and Kohn [4]. This theorem is frequently, more or less explicitly, used in the papers on minimum compliance of 2D bodies, cf. Bendsøe ([6] and the literature given therein), Bendsøe and Sigmund [7]. Using 2nd rank laminates has the virtue of dealing with explicit, relatively simple formulae for the components of Hooke's tensor, which simplifies the sensitivity analysis and makes it possible to use COC algorithms. The problem of minimal compliance of thin plates in bending can also be solved with using 2nd rank (not necessarily orthogonal) laminates, called here ribbed plates, as proved by Gibiansky and Cherkaev [21]. This theoretical result applies in numerical algorithms, see Czarnecki and Lewiński [12], Czarnecki *et al.* [10, 11].

In the present paper we apply this method for two-component 3D minimum compliance problem. Originally, the minimum compliance problem was called: designing for minimum of elastic potential, see Wasiutyński [37]. The numerical approach could have been performed thank of having at our disposal the explicit formulae for the moduli of 3rd rank stiff laminates. The derivation is reported here; it is based upon the Francfort-Murat formula [19]. The available literature on the layout problems of 3D bodies concerns shape design or the case of the weaker material being degenerated to voids ($\kappa_1 = 0$, $\mu_1 = 0$), since only for this special case the explicit formulae for the components of the effective Hooke's tensor were available, see Krog and Olhoff [26], Eschenauer and Olhoff [18], Jacobsen *et al.* [23].

The present paper extends our previous results announced at CMM Conference, see Czarnecki and Lewiński [13]. The 3D minimum compliance problem (for two-component design) has also been considered in Díaz and Lipton [14] but the approach is there different, with using so called moment formulation, see Francfort *et al.* [20].

The relaxed formulation based on the homogenization results of the stiffest design problem considered here is now rarely adopted in the literature targeted at finding practical numerical results. The main stream of pragmatic works concerns rather the shape design problem (one phase design) for which a special, rather approximate effective constitutive relation is adopted, called a power-law, see Olhoff *et al.* [35], Bendsøe and Sigmund [7], Borrvall and Petersson [8], Kutyłowski [27], Marczewska *et al.* [30].

The advantage of using the relaxation by homogenization approach lies in its mathematical correctness, clarity and theoretical importance. Moreover, the solutions turn out to be stable and reliable, not exhibiting special checkerboard patterns.

The following conventions are adopted: small Greek indices take values 1 and 2, the small Latin indices i, j, k, l, m, n take values 1, 2 and 3, while the indices a and b run over 1,...,6. The finite elements are indexed by $e = 1, \ldots, N$. The summation convention is adopted for repeated indices.

2. Minimum compliance problem in 3D. The initial non-relaxed formulation

The classical problem of forming the stiffest structure within a given feasible domain can be formulated as follows. Assume that the feasible 3D domain Ω is parametrized by the Cartesian coordinate system (x_1, x_2, x_3) with the orthonormal basis $(\mathbf{e}_1, \mathbf{e}_2, \mathbf{e}_3)$. A part Γ_u of $\partial\Omega$ is considered as a support, where the displacement field $\mathbf{u} = (u_1, u_2, u_3)$ vanishes. The remaining part Γ_t of the boundary $\partial\Omega$ is subjected to given tractions $\mathbf{t} = (t_1, t_2, t_3)$, while the density of the body forces form a field $\mathbf{p} = (p_1, p_2, p_3)$ within Ω. The domain Ω must be filled up with two isotropic materials characterized by the Hooke's law,

$$\sigma_{ij} = C^{\alpha}_{ijkl}\varepsilon_{kl}, \qquad \alpha = 1, 2, \quad i, j, k, l = 1, 2, 3, \tag{1}$$

where $\boldsymbol{\sigma} = (\sigma_{ij})$ represents the stress tensor field; $\boldsymbol{\varepsilon} = (\varepsilon_{ij})$ represents the strain field defined as in the linear theory of elasticity,

$$\varepsilon_{ij}(\mathbf{u}) = \frac{1}{2}\left(\frac{\partial u_i}{\partial x_j} + \frac{\partial u_j}{\partial x_i}\right), \tag{2}$$

and the elasticity tensors $\mathbf{C}^{\alpha}$, for $\alpha = 1, 2$, are isotropic

$$\mathbf{C}^{\alpha} = 2\mu_{\alpha}\mathbf{P}_s + 3\kappa_{\alpha}\mathbf{P}_h. \tag{3}$$

Here, μ_{α}, κ_{α} are the bulk and shear moduli of the αth phase and $\mathbf{P}_s$, $\mathbf{P}_h$ are projection operators onto the deviatoric and hydrostatic strains, respectively, see Lipton [29], Rychlewski [36]. Their representations are

$$\mathbf{P}_h = (\mathbf{P}_h)_{ijkl}\,\mathbf{e}_i \otimes \mathbf{e}_j \otimes \mathbf{e}_k \otimes \mathbf{e}_l, \tag{4}$$

$$\mathbf{P}_s = (\mathbf{P}_s)_{ijkl}\,\mathbf{e}_i \otimes \mathbf{e}_j \otimes \mathbf{e}_k \otimes \mathbf{e}_l, \tag{5}$$

where

$$(\mathbf{P}_h)_{ijkl} = \frac{1}{3}\delta_{ij}\delta_{kl}\,, \tag{6}$$

$$(\mathbf{P}_s)_{ijkl} = \frac{1}{2}\left(\delta_{ik}\delta_{jl} + \delta_{il}\delta_{jk}\right) - \frac{1}{3}\delta_{ij}\delta_{kl}\,. \tag{7}$$

The moduli μ_α, κ_α are linked with the Young moduli E_α and Poisson's ratios ν_α by the formulae

$$\kappa_\alpha = \frac{E_\alpha}{3\,(1-2\nu_\alpha)}\,, \qquad \mu_\alpha = \frac{E_\alpha}{2\,(1+\nu_\alpha)}\,. \tag{8}$$

It is assumed that the second material is stronger, or

$$\kappa_1 < \kappa_2\,, \qquad \mu_1 < \mu_2\,. \tag{9}$$

The field $\mathbf{u}$ is looked for within the space U of trial kinematically admissible displacement fields which are sufficiently regular and vanish on Γ_u. This field satisfies the variational equation of equilibrium

$$a(\mathbf{u},\mathbf{v}) = f(\mathbf{v}) \quad \forall \mathbf{v} \in U \tag{10}$$

where

$$a(\mathbf{u},\mathbf{v}) = \int_\Omega C_{ijkl}(\mathbf{x})\,\varepsilon_{ij}(\mathbf{u})\,\varepsilon_{kl}(\mathbf{v})\,\mathrm{d}\Omega \tag{11}$$

and

$$f(\mathbf{v}) = \int_\Omega \mathbf{p}\cdot\mathbf{v}\,\mathrm{d}\Omega + \int_{\Gamma_t} \mathbf{t}\cdot\mathbf{v}\,\mathrm{d}\Gamma\,. \tag{12}$$

Here $\mathbf{C} = (C_{ijkl})$ assumes the form $\mathbf{C}^1$ or $\mathbf{C}^2$. Let the second material occupies a subdomain Ω_2 and we assume that its volume is prescribed as V_2,

$$\int_{\Omega_2} \mathrm{d}\Omega = V_2\,. \tag{13}$$

The stiffest design problem consists in finding a minimizer of the compliance $f(\mathbf{u})$ among all admissible distributions of the phases satisfying the isoperimetric condition (13),

$$(P_0) \qquad \min_{\substack{\mathbf{C}(x)\\ \text{subject to (10)}-\text{(13)}}} f(\mathbf{u})\,. \tag{14}$$

It is known that the above problem requires relaxation, see Lipton [29], Cherkaev [9] and Allaire [2]. According to the Theorem 4.1.12 in Allaire [2] the problem P_0 should be reformulated as follows:

a) tensor $\mathbf{C}$ should refer to so-called stiff (or strong) orthotropic laminates of third rank; their construction will be explained in the sequel,

b) the isoperimetric condition (13) should concern the distribution of the stronger phase of the composite considered.

Upon relaxation the problem will be called (P). The changes (a, b) suffice to make this problem well posed. The present paper is based on this relaxed formulation.

Prior to putting forward the relaxed formulation (P) in greater detail we consider now the effective properties of the 3rd rank stiff laminates.

3. The iterative formula for the effective moduli tensor of two-phase laminates

An iterative formula for effective moduli of laminates composed of two constituents has been first derived by Francfort and Murat [19]. This formula makes it possible to find the effective moduli of laminates of higher rank which are widely used in the optimization theory of elastic bodies, see Cherkaev [9]. To be specific, assume that two elastic materials are stacked together: one of arbitrary moduli tensor $\mathbf{C}^1$ and second one isotropic of moduli tensor $\mathbf{C}^2$ determined by the bulk modulus κ_2 and the shear modulus μ_2. We assume that $\mathbf{C^2} - \mathbf{C^1}$ is invertible. The lamination direction is determined by a unit vector $\mathbf{n}$; the volume fractions of the materials are θ_1 and θ_2, respectively, see Fig. 1. The iterative formula for the homogenized tensor $\mathbf{C}^h$ reads

$$\theta_1(\mathbf{C}^2 - \mathbf{C}^h)^{-1} = (\mathbf{C}^2 - \mathbf{C}^1)^{-1} - \theta_2\mathbf{\Gamma}^2 \tag{15}$$

and the 4th rank tensor $\mathbf{\Gamma}^2$ depends on κ_2, μ_2 and $\mathbf{n}$. It has the form

$$\Gamma^2_{ijkl} = \frac{1}{4\mu_2}(\delta_{ki}n_ln_j + \delta_{li}n_kn_j + \delta_{kj}n_ln_i + \delta_{lj}n_kn_i) - \frac{(3\kappa_2 + \mu_2)}{\mu_2(3\kappa_2 + 4\mu_2)} n_ln_kn_in_j\,. \tag{16}$$

Action of $\mathbf{\Gamma}^2$ on a second order tensor can be given by a formula (4.34) of [19]. Nevertheless, the representation (16) is not reported in Francfort and Murat [19]. Since the derivation of (15) given in the latter paper is highly mathematical it is thought appropriate to put below a simplified derivation of this important formula, see also Kohn [25]. The two-dimensional counterpart of (15) is reported in Lewiński and Telega [28].

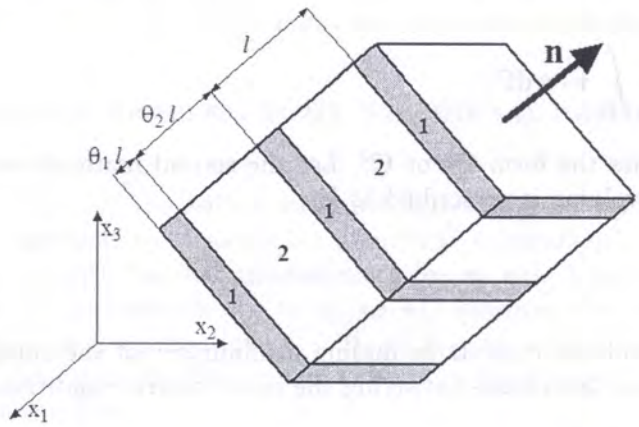

Fig. 1. First rank two-material laminate

In the case considered all auxiliary fields involved in the basic cell problem for the laminate of Fig.1 are piecewise constant, with possible jumps along the material interface. In particular, the stresses are equal to (σ^1_{ij}) in the domain occupied by the material 1 and equal to (σ^2_{ij}) in the domain occupied by material 2. The averaged stress field (σ^h_{ij}) is defined by

$$\sigma^h_{ij} = \theta_1\sigma^1_{ij} + \theta_2\sigma^2_{ij}\,, \qquad \theta_1 + \theta_2 = 1, \tag{17}$$

a similar equation for strains has the form

$$\varepsilon^h_{ij} = \theta_1\varepsilon^1_{ij} + \theta_2\varepsilon^2_{ij} \tag{18}$$

and the constitutive equations are

$$\sigma^1_{ij} = C^1_{ijkl}\varepsilon^1_{kl}\,, \qquad \sigma^2_{ij} = C^2_{ijkl}\varepsilon^2_{kl}\,. \tag{19}$$

We assume that $\mathbf{C}^2$ is isotropic, hence

$$\mathbf{C}^2 = 2\mu_2 \mathbf{P}_s + 3\kappa_2 \mathbf{P}_h \tag{20}$$

where $\mathbf{P}_s$, $\mathbf{P}_h$ are given by Eqs. (4)–(7).

The continuity conditions along the interface between both the materials are

$$\sigma^1_{ij} n_j \quad = \sigma^2_{ij} n_j \,, \tag{21}$$

$$\varepsilon^1_{ij} - \varepsilon^2_{ij} = p_i n_j + n_i p_j \,. \tag{22}$$

Here, $\mathbf{p}$ is an arbitrary vector. Equations (17)–(22) imply (15), (16), where $\mathbf{C}^h$ links $\boldsymbol{\sigma}^h$ and $\boldsymbol{\varepsilon}^h$ by

$$\boldsymbol{\sigma}^h = \mathbf{C}^h \boldsymbol{\varepsilon}^h. \tag{23}$$

We shall show this passage in several elementary steps. Note that Eqs. (17), (19), (23) imply

$$\mathbf{C}^h \boldsymbol{\varepsilon}^h = \theta_1 \mathbf{C}^1 \boldsymbol{\varepsilon}^1 + \theta_2 \mathbf{C}^2 \boldsymbol{\varepsilon}^2, \tag{24}$$

but, by Eq. (18),

$$\theta_2 \boldsymbol{\varepsilon}^2 = \boldsymbol{\varepsilon}^h - \theta_1 \boldsymbol{\varepsilon}^1. \tag{25}$$

Hence

$$\mathbf{C}^h \boldsymbol{\varepsilon}^h = \theta_1 \mathbf{C}^1 \boldsymbol{\varepsilon}^1 + \mathbf{C}^2 (\boldsymbol{\varepsilon}^h - \theta_1 \boldsymbol{\varepsilon}^1) \tag{26}$$

or

$$(\mathbf{C}^2 - \mathbf{C}^h)\, \boldsymbol{\varepsilon}^h = \theta_1 \mathbf{N} \tag{27}$$

with

$$\mathbf{N} = (\mathbf{C}^2 - \mathbf{C}^1)\, \boldsymbol{\varepsilon}^1. \tag{28}$$

We can write

$$\boldsymbol{\varepsilon}^1 = (\mathbf{C}^2 - \mathbf{C}^1)^{-1} \mathbf{N}, \qquad \boldsymbol{\varepsilon}^h = \theta_1 (\mathbf{C}^2 - \mathbf{C}^h)^{-1} \mathbf{N}, \tag{29}$$

since $(\mathbf{C}^2 - \mathbf{C}^1)$ is assumed as invertible. Substitution of Eq. (22) into (18) gives

$$\boldsymbol{\varepsilon}^h = \theta_1 \boldsymbol{\varepsilon}^1 + \theta_2 \left(\boldsymbol{\varepsilon}^1 - \mathbf{p} \otimes \mathbf{n} - \mathbf{n} \otimes \mathbf{p}\right) \tag{30}$$

or

$$\boldsymbol{\varepsilon}^h = \boldsymbol{\varepsilon}^1 - \theta_2 (\mathbf{p} \otimes \mathbf{n} + \mathbf{n} \otimes \mathbf{p}). \tag{31}$$

By (29) we can write Eq. (31) in the form

$$\theta_1 (\mathbf{C}^2 - \mathbf{C}^h)^{-1} \mathbf{N} = (\mathbf{C}^2 - \mathbf{C}^1)^{-1} \mathbf{N} - \theta_2 (\mathbf{p} \otimes \mathbf{n} + \mathbf{n} \otimes \mathbf{p}). \tag{32}$$

To prove (15) it is sufficient to express $\mathbf{p}$ in terms of $\mathbf{N}$. To this end we make use of Eq. (21),

$$C^1_{ijkl} \varepsilon^1_{kl} n_j = C^2_{ijkl} \varepsilon^2_{kl} n_j \,. \tag{33}$$

Substitution of Eq. (22) gives

$$C^1_{ijkl} \varepsilon^1_{kl} n_j = C^2_{ijkl} \left(\varepsilon^1_{kl} - p_k n_l - n_k p_l\right) n_j \,, \tag{34}$$

which can be put in the form

$$C^2_{ijkl} \left(p_k n_l + n_k p_l\right) n_j = N_{ij} n_j \,. \tag{35}$$

with $\mathbf{N}$ given by Eq. (28). Equation (35) reads

$$\left(2C^2_{ijkl}n_l n_j\right) p_k = N_{ij}n_j \,. \tag{36}$$

Let us compute

$$C^2_{ijkl}n_l n_j = \mu_2\delta_{ik} + \left(\kappa_2 + \frac{1}{3}\mu_2\right) n_i n_k \,. \tag{37}$$

Hence Eq. (36) assumes the form

$$\mu_2 p_i + \left(\kappa_2 + \frac{1}{3}\mu_2\right)(\mathbf{p}\cdot\mathbf{n})\, n_i = \frac{1}{2}N_{ij}n_j \,. \tag{38}$$

By contracting with n_i we find

$$\mathbf{p}\cdot\mathbf{n} = \frac{3}{6\kappa_2 + 8\mu_2}\left(N_{kl}n_k n_l\right) \tag{39}$$

and come back to Eq. (38) to find

$$\mu_2 p_i = \frac{1}{2}N_{ij}n_j - \frac{3\kappa_2 + \mu_2}{6\kappa_2 + 8\mu_2}\left(N_{kl}n_k n_l\right) n_i \,. \tag{40}$$

Hence we find the expression

$$\mu_2\left(p_i n_j + p_j n_i\right) = \frac{1}{2}N_{lk}\delta_{li}n_k n_j + \frac{1}{2}N_{lk}\delta_{lj}n_k n_i - \frac{3\kappa_2 + \mu_2}{3\kappa_2 + 4\mu_2}\left(N_{kl}n_k n_l\right) n_i n_j \,. \tag{41}$$

Now we symmetrize the right-hand side of Eq. (41)

$$\mu_2(p_i n_j + p_j n_i) = \left\{\frac{1}{4}\left(\delta_{ki}n_l n_j + \delta_{li}n_k n_j + \delta_{kj}n_l n_i + \delta_{lj}n_k n_i\right) - \frac{3\kappa_2 + \mu_2}{3\kappa_2 + 4\mu_2}\, n_i n_j n_k n_l\right\} N_{kl} \,. \tag{42}$$

Using the tensor (16) one finds

$$p_i n_j + p_j n_i = \Gamma^2_{ijkl}N_{kl} \tag{43}$$

or

$$\mathbf{p}\otimes\mathbf{n} + \mathbf{n}\otimes\mathbf{p} = \boldsymbol{\Gamma}^2\mathbf{N}. \tag{44}$$

Substitution into Eq. (32) gives

$$\left[\theta_1(\mathbf{C}^2 - \mathbf{C}^h)^{-1} - (\mathbf{C}^2 - \mathbf{C}^1)^{-1} + \theta_2\boldsymbol{\Gamma}^2\right]\mathbf{N} = \mathbf{0}. \tag{45}$$

The quantities ε^1_{ij} can be viewed as arbitrary and the property of $(\mathbf{C}^2 - \mathbf{C}^1)$ being invertible means that $\mathbf{N}$ is arbitrary and Eq. (45) implies Eq. (15). The case when the set

$$\left\{\boldsymbol{\varepsilon} \;\middle|\; \varepsilon_{ij}\left(C^2_{ijkl} - C^1_{ijkl}\right)\varepsilon_{kl} = 0\right\}$$

has elements different from zero should be treated separately, see Francfort and Murat [19].

The case of a $\mathbf{C}^2$ being anisotropic is tractable, but the final result is less elegant.

4. EXPLICT FORMULAE FOR COMPONENTS OF THE EFFECTIVE TENSOR OF STIFF 3RD LAMINATES

As explained in the Introduction the minimum compliance problem must be relaxed by admitting composite domains of so called stiff laminates of 3rd rank. Formation of the stiff laminate of the third rank is explained in Fig. 2. In the first step both the phases (of volume fractions θ_1 and θ_2) are stacked to form a laminate into the direction of a unit vector $\mathbf{n}_1$. This laminate will be referred to as the "h" laminate. In the second step we mix the material "h" with material "2" (with volume fractions α_1 and α_2, respectively) along the direction of the unit vector $\mathbf{n}_2$, orthogonal to $\mathbf{n}_1$. The laminate "hh" thus obtained is mixed once again with material "2" – note that this is the stiffer material - with a new laminate direction $\mathbf{n}_3$ (orthogonal to both the vectors $\mathbf{n}_1$ and $\mathbf{n}_2$) with volume fractions β_1 and β_2 for the "hh" and the "2" phases, respectively. Thus the "hhh" laminated composite emerges.

We derive now the explicit formulae for the effective moduli of the stiff third rank laminate of Fig. 2. The first step is to mix two isotropic materials of the bulk moduli κ_α and the shear moduli μ_α, $\alpha = 1, 2$, to construct a laminate with area fractions θ_α; the unit vector $\mathbf{n}$ is perpendicular to the planes of stitching both the materials. The effective moduli tensor is given by Eq. (15), where

$$\mathbf{\Gamma}^2 = \frac{1}{\mu_2}\,\mathbf{\Psi}(\mathbf{n}) \tag{46}$$

and

$$(\mathbf{\Psi}(\mathbf{n}))_{ijkl} = \frac{1}{4}\,(\delta_{ki}n_l n_j + \delta_{li}n_k n_j + \delta_{kj}n_l n_i + \delta_{lj}n_k n_i) - \psi\; n_i n_j n_k n_l \tag{47}$$

where

$$\psi = \frac{3\kappa_2 + \mu_2}{3\kappa_2 + 4\mu_2}\,, \qquad \psi = \frac{1}{2(1-\nu_2)}\,. \tag{48}$$

Tensor $\mathbf{C}^2$ is given by Eq. (20) and the formula for $\mathbf{C}^1$ is similar. Let us assume that $\mathbf{n} = (1, 0, 0)$, or $\mathbf{n} = \mathbf{n}_1$, $\mathbf{n}_1$ being the first basis vector.

In the next step we mix the material thus obtained (with moduli C^h_{ijkl}) once again with the material 2 of moduli C^2_{ijkl}; we take the volume fractions: α_1, α_2, and take $\mathbf{n} = (0, 1, 0)$ or $\mathbf{n} = \mathbf{n}_2$. We say that the material 2 is an envelope. The effective moduli tensor, denoted by $\mathbf{C}^{hh}$ is determined by the rule (15),

$$\alpha_1\,(\mathbf{C}^2 - \mathbf{C}^{hh})^{-1} = (\mathbf{C}^2 - \mathbf{C}^h)^{-1} - \frac{\alpha_2}{\mu_2}\,\mathbf{\Psi}(\mathbf{n}_2)\,. \tag{49}$$

Hence

$$\alpha_1\theta_1\,(\mathbf{C}^2 - \mathbf{C}^{hh})^{-1} = (\mathbf{C}^2 - \mathbf{C}^1)^{-1} - \frac{1}{\mu_2}\,[\theta_2\mathbf{\Psi}(\mathbf{n}_1) + \theta_1\alpha_2\mathbf{\Psi}(\mathbf{n}_2)]\,. \tag{50}$$

In the last step we mix the $\mathbf{C}^{hh}$ material with the material $\mathbf{C}^2$ in proportions β_1 and β_2, respectively. We take now $\mathbf{n} = \mathbf{n}_3 = (0, 0, 1)$. Thus the effective moduli tensor $\mathbf{C}^{hhh}$ is given by

$$m_1\,(\mathbf{C}^2 - \mathbf{C}^{hhh})^{-1} = (\mathbf{C}^2 - \mathbf{C}^1)^{-1} - \frac{1}{\mu_2}\,\mathbf{\Psi} \tag{51}$$

with $m_1 = \theta_1\alpha_1\beta_1$ and

$$\mathbf{\Psi} = \theta_2\,\mathbf{\Psi}(\mathbf{n}_1) + \alpha_2\theta_1\,\mathbf{\Psi}(\mathbf{n}_2) + \beta_2\alpha_1\theta_1\,\mathbf{\Psi}(\mathbf{n}_3) \tag{52}$$

or

$$\mathbf{\Psi} = \sum_{i=1}^{3} \rho_i\,\mathbf{\Psi}(\mathbf{n}_i), \qquad \rho_1 = \theta_2\,, \qquad \rho_2 = \alpha_2\theta_1\,, \qquad \rho_3 = \beta_2\alpha_1\theta_1\,. \tag{53}$$

We note that $\rho_1 + \rho_2 + \rho_3 = 1 - m_1 = m_2$, m_α being the resulting volume fraction of the αth material.

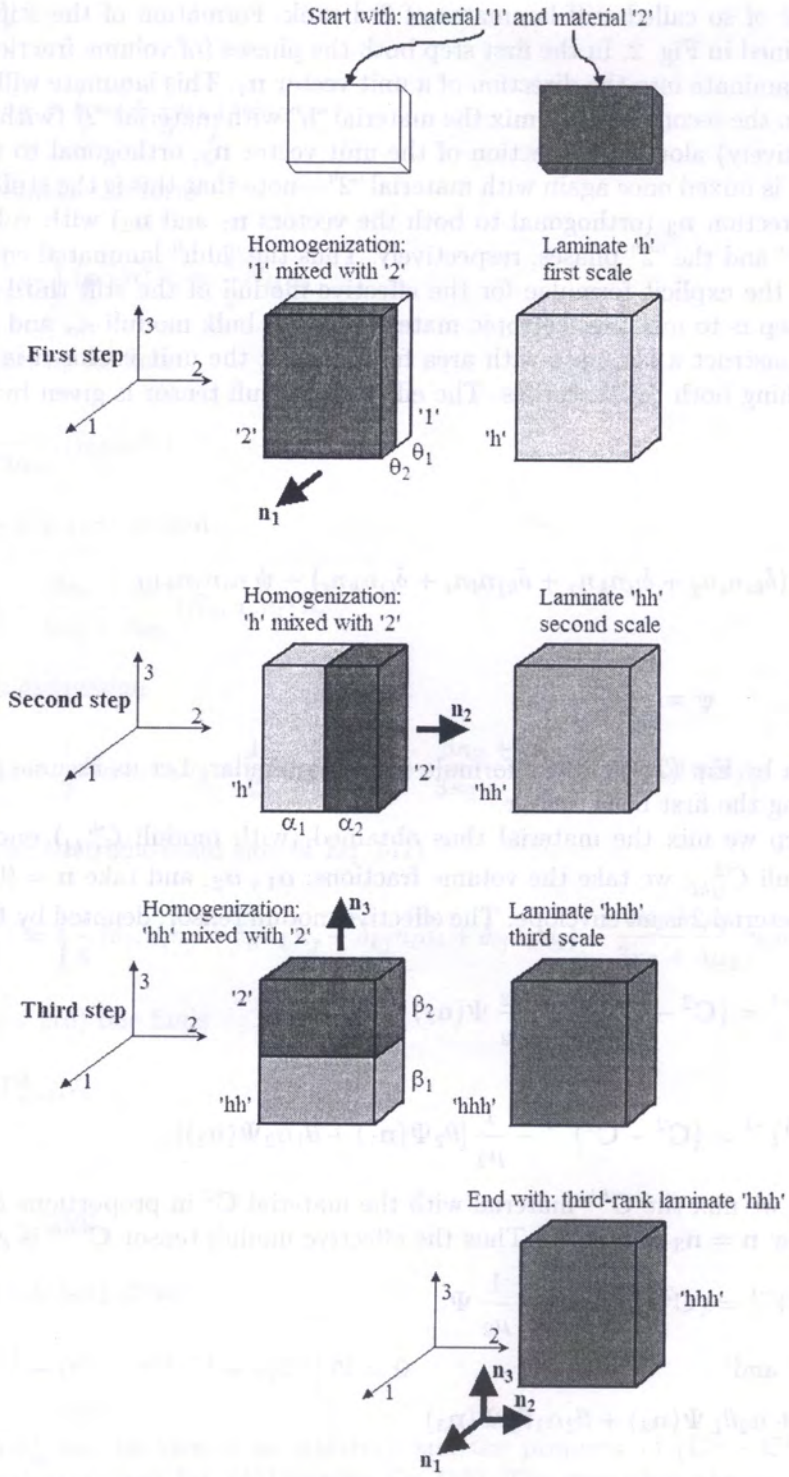

Fig. 2. Construction of the third rank strong laminate

Computing the moduli $\mathbf{C}^{hhh}$ *referred to* $(\mathbf{n}_i)$

We introduce the basis, see Cherkaev [9, Eq. 14.3.11], and Jemioło and Szwed [24, p. 43],

$$\begin{aligned}
&\mathbf{a}_i = \mathbf{n}_i \otimes \mathbf{n}_i\,, \quad i = 1,2,3,\\
&\mathbf{a}_4 = \tfrac{1}{\sqrt{2}}(\mathbf{n}_2 \otimes \mathbf{n}_3 + \mathbf{n}_3 \otimes \mathbf{n}_2),\\
&\mathbf{a}_5 = \tfrac{1}{\sqrt{2}}(\mathbf{n}_1 \otimes \mathbf{n}_3 + \mathbf{n}_3 \otimes \mathbf{n}_1),\\
&\mathbf{a}_6 = \tfrac{1}{\sqrt{2}}(\mathbf{n}_2 \otimes \mathbf{n}_1 + \mathbf{n}_1 \otimes \mathbf{n}_2).
\end{aligned} \tag{54}$$

(do not sum over i). We refer the projection operators $\mathbf{P}_h$, $\mathbf{P}_s$, Eqs. (4), (5), to the basis (54):

$$\mathbf{P}_h = \sum_{b,d=1}^{6} (\mathbf{P}_h)_{bd}\, \mathbf{a}_b \otimes \mathbf{a}_d, \qquad \mathbf{P}_s = \sum_{b,d=1}^{6} (\mathbf{P}_s)_{bd}\, \mathbf{a}_b \otimes \mathbf{a}_d \tag{55}$$

and find the matrices

$$[(\mathbf{P}_h)_{bd}] = \begin{vmatrix} 1/3 & 1/3 & 1/3 & 0 & 0 & 0 \\ 1/3 & 1/3 & 1/3 & 0 & 0 & 0 \\ 1/3 & 1/3 & 1/3 & 0 & 0 & 0 \\ 0 & 0 & 0 & 0 & 0 & 0 \\ 0 & 0 & 0 & 0 & 0 & 0 \\ 0 & 0 & 0 & 0 & 0 & 0 \end{vmatrix}, \qquad [(\mathbf{P}_s)_{bd}] = \begin{vmatrix} 2/3 & -1/3 & -1/3 & 0 & 0 & 0 \\ -1/3 & 2/3 & -1/3 & 0 & 0 & 0 \\ -1/3 & -1/3 & 2/3 & 0 & 0 & 0 \\ 0 & 0 & 0 & 1 & 0 & 0 \\ 0 & 0 & 0 & 0 & 1 & 0 \\ 0 & 0 & 0 & 0 & 0 & 1 \end{vmatrix}. \tag{56}$$

We easy check the well-known properties of the projectors

$$\begin{aligned}
&\mathbf{P}_h\mathbf{P}_s = \mathbf{0}, \qquad \mathbf{P}_s\mathbf{P}_h = \mathbf{0}, \qquad \mathbf{P}_h\mathbf{P}_h = \mathbf{P}_h\,, \qquad \mathbf{P}_s\mathbf{P}_s = \mathbf{P}_s\,,\\
&\mathbf{P}_h + \mathbf{P}_s = \mathbf{I} = \mathrm{diag}[1,1,1,1,1,1].
\end{aligned} \tag{57}$$

Moreover, we introduce the representations

$$\mathbf{\Psi} = \sum_{b,d=1}^{6} (\mathbf{\Psi})_{bd}\, \mathbf{a}_b \otimes \mathbf{a}_d\,, \qquad \mathbf{C}^{\alpha} = \sum_{b,d=1}^{6} (\mathbf{C}^{\alpha})_{bd}\, \mathbf{a}_b \otimes \mathbf{a}_d\,, \qquad \alpha = 1,2, \tag{58}$$

where the components are

$$[(\mathbf{\Psi})_{bd}] = \mathrm{diag}\left[(1-\psi)\rho_1\,,\, (1-\psi)\rho_2\,,\, (1-\psi)\rho_3\,,\, \frac{1}{2}(\rho_2+\rho_3)\,,\, \frac{1}{2}(\rho_1+\rho_3)\,,\, \frac{1}{2}(\rho_2+\rho_1)\right], \tag{59}$$

and

$$[(\mathbf{C}^{\alpha})_{bd}] = \begin{vmatrix} G_\alpha & H_\alpha & H_\alpha & 0 & 0 & 0 \\ H_\alpha & G_\alpha & H_\alpha & 0 & 0 & 0 \\ H_\alpha & H_\alpha & G_\alpha & 0 & 0 & 0 \\ 0 & 0 & 0 & 2\mu_\alpha & 0 & 0 \\ 0 & 0 & 0 & 0 & 2\mu_\alpha & 0 \\ 0 & 0 & 0 & 0 & 0 & 2\mu_\alpha \end{vmatrix} \tag{60}$$

with

$$G_\alpha = \kappa_\alpha + \frac{4}{3}\mu_\alpha\,, \qquad H_\alpha = \kappa_\alpha - \frac{2}{3}\mu_\alpha\,, \qquad \alpha = 1,2. \tag{61}$$

The first term in the right-hand side of Eq. (50) reads

$$\left(\mathbf{C}^2 - \mathbf{C}^1\right)^{-1} = \frac{1}{2\Delta\mu}\,\mathbf{P}_s + \frac{1}{3\Delta\kappa}\,\mathbf{P}_h \tag{62}$$

with $\Delta\mu = \mu_2 - \mu_1$, $\Delta\kappa = \kappa_2 - \kappa_1$. Let us define the quantities

$$\tilde{\kappa} = \Delta\kappa/G_2\,, \qquad \tilde{\mu} = \Delta\mu/G_2\,, \tag{63}$$

and the functions

$$D(x,y,z) = 36\tilde{\kappa}(\tilde{\mu})^2 xyz - 4\tilde{\mu}(\tilde{\mu}+3\tilde{\kappa})(xy+xz+yz) + (4\tilde{\mu}+3\tilde{\kappa})(x+y+z) - 3, \tag{64}$$

$$g(x,y) = -36\tilde{\kappa}(\tilde{\mu})^2 xy + 4\tilde{\mu}(\tilde{\mu}+3\tilde{\kappa})(x+y) - (4\tilde{\mu}+3\tilde{\kappa}), \tag{65}$$

$$b(x) = (3\tilde{\kappa}-2\tilde{\mu})(2\tilde{\mu}\,x - 1), \tag{66}$$

$$s(x,y,z) = 1 - (x+y+z). \tag{67}$$

By using the formula (51) we compute the components of tensor $\mathbf{C}^{hhh}$ referred to $(\mathbf{n}_i)$

$$\begin{aligned} C^{hhh}_{1111}/G_2 &= 1 - \frac{s(\rho_1,\rho_2,\rho_3)\,g(\rho_2,\rho_3)}{D(\rho_1,\rho_2,\rho_3)}\,, \\ C^{hhh}_{2222}/G_2 &= 1 - \frac{s(\rho_1,\rho_2,\rho_3)\,g(\rho_1,\rho_3)}{D(\rho_1,\rho_2,\rho_3)}\,, \\ C^{hhh}_{3333}/G_2 &= 1 - \frac{s(\rho_1,\rho_2,\rho_3)\,g(\rho_1,\rho_2)}{D(\rho_1,\rho_2,\rho_3)}\,, \end{aligned} \tag{68}$$

$$\begin{aligned} C^{hhh}_{1122} &= H_2 - \frac{s(\rho_1,\rho_2,\rho_3)\,b(\rho_3)}{D(\rho_1,\rho_2,\rho_3)}\,G_2\,, \\ C^{hhh}_{1133} &= H_2 - \frac{s(\rho_1,\rho_2,\rho_3)\,b(\rho_2)}{D(\rho_1,\rho_2,\rho_3)}\,G_2\,, \\ C^{hhh}_{2233} &= H_2 - \frac{s(\rho_1,\rho_2,\rho_3)\,b(\rho_1)}{D(\rho_1,\rho_2,\rho_3)}\,G_2\,, \end{aligned} \tag{69}$$

$$\begin{aligned} C^{hhh}_{1212} &= \mu_2 - s(\rho_1,\rho_2,\rho_3)\left[\frac{1}{\Delta\mu} - \frac{1}{\mu_2}(\rho_1+\rho_2)\right]^{-1}, \\ C^{hhh}_{1313} &= \mu_2 - s(\rho_1,\rho_2,\rho_3)\left[\frac{1}{\Delta\mu} - \frac{1}{\mu_2}(\rho_1+\rho_3)\right]^{-1}, \\ C^{hhh}_{2323} &= \mu_2 - s(\rho_1,\rho_2,\rho_3)\left[\frac{1}{\Delta\mu} - \frac{1}{\mu_2}(\rho_2+\rho_3)\right]^{-1}. \end{aligned} \tag{70}$$

Other components vanish or can be found by symmetry properties. We remember that, see Eq. (53), $\rho_1 = \theta_2$, $\rho_2 = \alpha_2(1-\theta_2)$, $\rho_3 = \beta_2(1-\alpha_2)(1-\theta_2)$, hence the volume fraction of the stiffer material is expressed by

$$m_2 = \theta_2 + \alpha_2 + \beta_2 - \theta_2\alpha_2 - \theta_2\beta_2 - \alpha_2\beta_2 + \theta_2\alpha_2\beta_2\,. \tag{71}$$

We shall find the components C_{ijkl} of tensor $\mathbf{C}^{hhh}$

$$\mathbf{C}^{hhh} = C_{ijkl}\,\mathbf{e}_i \otimes \mathbf{e}_j \otimes \mathbf{e}_k \otimes \mathbf{e}_l\,, \tag{72}$$

where $(\mathbf{e}_1, \mathbf{e}_2, \mathbf{e}_3)$ are basis vectors not coinciding, in general, with the vectors $(\mathbf{n}_1, \mathbf{n}_2, \mathbf{n}_3)$. Alternatively,

$$\mathbf{C}^{hhh} = C^{hhh}_{ijkl}\,\mathbf{n}_i \otimes \mathbf{n}_j \otimes \mathbf{n}_k \otimes \mathbf{n}_l \tag{73}$$

where C^{hhh}_{ijkl} are given by Eqs. (68)–(70).

The vectors $(\mathbf{n}_1, \mathbf{n}_2, \mathbf{n}_3)$ can be treated as a result of rotation of the basis $(\mathbf{e}_1, \mathbf{e}_2, \mathbf{e}_3)$. We define the matrix

$$\mathbf{Q} = \begin{bmatrix} \mathbf{n}_1^T \\ \mathbf{n}_2^T \\ \mathbf{n}_3^T \end{bmatrix}. \tag{74}$$

The following relation holds

$$\mathbf{n}_i = Q_{ij}\mathbf{e}_j, \qquad i,j = 1,2,3, \tag{75}$$

the matrix $\mathbf{Q}$ being orthogonal. The representation, see Eq. (72),

$$\mathbf{C}^{hhh} = C_{pqrs}\,\mathbf{e}_p \otimes \mathbf{e}_q \otimes \mathbf{e}_r \otimes \mathbf{e}_s \tag{76}$$

determines the relation

$$C_{pqrs} = Q_{ip}Q_{jq}Q_{kr}Q_{ls}C^{hhh}_{ijkl}. \tag{77}$$

To make the computations easier we reformulate the relation above to the matrix form

$$\left[\hat{C}_{ab}\right] = \hat{\mathbf{Q}}^T \left[\hat{C}^{hhh}_{ab}\right] \hat{\mathbf{Q}}, \qquad a,b = 1,\ldots,6, \tag{78}$$

where

$$\left[\hat{C}^{hhh}_{ab}\right] = \begin{bmatrix} C^{hhh}_{1111} & C^{hhh}_{1122} & C^{hhh}_{1133} & 0 & 0 & 0 \\ & C^{hhh}_{2222} & C^{hhh}_{2233} & 0 & 0 & 0 \\ & & C^{hhh}_{3333} & 0 & 0 & 0 \\ & & & 2C^{hhh}_{2323} & 0 & 0 \\ & & & & 2C^{hhh}_{1313} & 0 \\ & & & & & 2C^{hhh}_{1212} \end{bmatrix} \tag{79}$$

and $\hat{\mathbf{Q}} = \left[\hat{Q}_{ab}\right]$, where, see Mehrabadi and Cowin [31],

$$\begin{aligned}
&\hat{Q}_{11} = (Q_{11})^2, && \hat{Q}_{21} = (Q_{21})^2, && \hat{Q}_{31} = (Q_{31})^2, \\
&\hat{Q}_{12} = (Q_{12})^2, && \hat{Q}_{22} = (Q_{22})^2, && \hat{Q}_{32} = (Q_{32})^2, \\
&\hat{Q}_{13} = (Q_{13})^2, && \hat{Q}_{23} = (Q_{23})^2, && \hat{Q}_{33} = (Q_{33})^2, \\
&\hat{Q}_{14} = \sqrt{2}Q_{12}Q_{13}, && \hat{Q}_{24} = \sqrt{2}Q_{22}Q_{23}, && \hat{Q}_{34} = \sqrt{2}Q_{33}Q_{32}, \\
&\hat{Q}_{15} = \sqrt{2}Q_{11}Q_{13}, && \hat{Q}_{25} = \sqrt{2}Q_{21}Q_{23}, && \hat{Q}_{35} = \sqrt{2}Q_{33}Q_{31}, \\
&\hat{Q}_{16} = \sqrt{2}Q_{11}Q_{12}, && \hat{Q}_{26} = \sqrt{2}Q_{22}Q_{21}, && \hat{Q}_{36} = \sqrt{2}Q_{31}Q_{32}, \\
&\hat{Q}_{41} = \sqrt{2}Q_{21}Q_{31}, && \hat{Q}_{51} = \sqrt{2}Q_{11}Q_{31}, && \hat{Q}_{61} = \sqrt{2}Q_{11}Q_{21}, \\
&\hat{Q}_{42} = \sqrt{2}Q_{22}Q_{32}, && \hat{Q}_{52} = \sqrt{2}Q_{12}Q_{32}, && \hat{Q}_{62} = \sqrt{2}Q_{12}Q_{22}, \\
&\hat{Q}_{43} = \sqrt{2}Q_{23}Q_{33}, && \hat{Q}_{53} = \sqrt{2}Q_{13}Q_{33}, && \hat{Q}_{63} = \sqrt{2}Q_{13}Q_{23}, \\
&\hat{Q}_{44} = Q_{22}Q_{33} + Q_{23}Q_{32}, && \hat{Q}_{54} = Q_{12}Q_{33} + Q_{32}Q_{13}, && \hat{Q}_{64} = Q_{12}Q_{23} + Q_{22}Q_{13}, \\
&\hat{Q}_{45} = Q_{21}Q_{33} + Q_{31}Q_{23}, && \hat{Q}_{55} = Q_{11}Q_{33} + Q_{13}Q_{31}, && \hat{Q}_{65} = Q_{11}Q_{23} + Q_{21}Q_{13}, \\
&\hat{Q}_{46} = Q_{21}Q_{32} + Q_{31}Q_{22}, && \hat{Q}_{56} = Q_{11}Q_{32} + Q_{31}Q_{12}, && \hat{Q}_{66} = Q_{11}Q_{22} + Q_{21}Q_{12}.
\end{aligned} \tag{80}$$

Note that the formula for $\hat{Q}_{61}$ in Ref. [31] is incorrect. Given the components $\hat{C}_{ab}$ one can find the components C_{ijkl} by the formulae

$$\begin{aligned}
&C_{1111} = \hat{C}_{11}, \\
&C_{1122} = \hat{C}_{21}, \quad C_{2222} = \hat{C}_{22}, \\
&C_{1133} = \hat{C}_{31}, \quad C_{2233} = \hat{C}_{32}, \quad C_{3333} = \hat{C}_{33}, \\
&C_{2311} = \tfrac{1}{\sqrt{2}}\hat{C}_{41}, \quad C_{2322} = \tfrac{1}{\sqrt{2}}\hat{C}_{42}, \quad C_{2333} = \tfrac{1}{\sqrt{2}}\hat{C}_{43}, \quad C_{2323} = \tfrac{1}{2}\hat{C}_{44}, \\
&C_{1311} = \tfrac{1}{\sqrt{2}}\hat{C}_{51}, \quad C_{1322} = \tfrac{1}{\sqrt{2}}\hat{C}_{52}, \quad C_{1333} = \tfrac{1}{\sqrt{2}}\hat{C}_{53}, \quad C_{1323} = \tfrac{1}{2}\hat{C}_{54}, \quad C_{1313} = \tfrac{1}{2}\hat{C}_{55}, \\
&C_{1211} = \tfrac{1}{\sqrt{2}}\hat{C}_{61}, \quad C_{1222} = \tfrac{1}{\sqrt{2}}\hat{C}_{62}, \quad C_{1233} = \tfrac{1}{\sqrt{2}}\hat{C}_{63}, \quad C_{1223} = \tfrac{1}{2}\hat{C}_{64}, \quad C_{1312} = \tfrac{1}{2}\hat{C}_{65}, \quad C_{1212} = \tfrac{1}{2}\hat{C}_{66};
\end{aligned} \tag{81}$$

other components can be found by symmetry properties

$$C_{ijmn} = C_{mnij}\,, \qquad C_{ijmn} = C_{jimn}\,, \qquad C_{ijmn} = C_{ijnm}\,, \qquad \text{for} \quad i,j,m,n = 1,2,3. \tag{82}$$

5. The relaxed formulation of the minimum compliance problem (P_0)

The relaxed formulation (P) for the original problem (P_0) is similar to (P_0) but now $\mathbf{C}$ is determined as explained in Sec. 4 (i.e. the moduli are given by Eq. (77)) and the constraint (13) is replaced by

$$\int_\Omega m_2 \,\mathrm{d}\Omega = V_2 \tag{83}$$

where $m_2(\mathbf{x})$ is expressed in terms of $\theta_2(\mathbf{x})$, $\alpha_2(\mathbf{x})$, $\beta_2(\mathbf{x})$ by Eq. (71). The design variables $\theta_2(\mathbf{x})$, $\alpha_2(\mathbf{x})$, $\beta_2(\mathbf{x})$, $\mathbf{x} \in \Omega$ satisfy the side conditions

$$0 \le \theta_2(\mathbf{x}) \le 1, \qquad 0 \le \alpha_2(\mathbf{x}), \qquad 0 \le \beta_2(\mathbf{x}) \le 1, \qquad \mathbf{x} \in \Omega. \tag{84}$$

The changes above were called (a,b), see Sec. 2, their mathematical justification being available in Allaire [2]. According to Theorem 4.1.12 in Allaire [2] the orthotropy directions $\mathbf{n}_i$ in the optimum solution of problem (P) follow trajectories of principal stresses. These trajectories coincide also with trajectories of strains. The only design variables of our problem are $\theta_2(\mathbf{x})$, $\alpha_2(\mathbf{x})$, $\beta_2(\mathbf{x})$, $\mathbf{x} \in \Omega$. The unit vectors $\mathbf{n}_i$ are eigenvectors of the stress state eigenvalue problem: find pairs $\left(\omega_i\,,\, \mathbf{v}^{(i)}\right)$ such that

$$\sum_{j=1}^{3} (\sigma_{kj} - \omega_i \delta_{kj})\, v_j^{(i)} = 0\,. \tag{85}$$

We write $\mathbf{n}_i = \mathbf{v}^{(i)} = (v_j^{(i)})$. Having found $\mathbf{n}_i$ we compose the matrix $\mathbf{Q}$ by Eq. (74) and determine the components of the effective Hooke's tensor as explained in Sec. 4.

6. Numerical solution by the COC method

To elaborate a numerical algorithm of solving problem (P) we use the Lagrange multipliers method along with the special updating schemes. The Lagrangian function takes the form, cf. Bendsøe [6]

$$\begin{aligned} L(\mathbf{v},\theta_2,\alpha_2,\beta_2) = {} & f(\mathbf{u}) - [a(\mathbf{u},\mathbf{v}) - f(\mathbf{v})] \\ & + \Lambda \left\{ \int_\Omega [\theta_2 + \alpha_2(1-\theta_2) + \beta_2(1-\alpha_2)(1-\theta_2)]\,\mathrm{d}\Omega - V_2 \right\} \\ & + \int_\Omega z^+_{\theta_2}(\theta_2 - 1)\,\mathrm{d}\Omega - \int_\Omega z^-_{\theta_2}\theta_2\,\mathrm{d}\Omega + \int_\Omega z^+_{\alpha_2}(\alpha_2 - 1)\,\mathrm{d}\Omega - \int_\Omega z^-_{\alpha_2}\alpha_2\,\mathrm{d}\Omega \\ & + \int_\Omega z^+_{\beta_2}(\beta_2 - 1)\,\mathrm{d}\Omega - \int_\Omega z^-_{\beta_2}\beta_2\,\mathrm{d}\Omega\,. \end{aligned} \tag{86}$$

The bilinear form $a(\cdot,\cdot)$ depends now on $\theta_2(\mathbf{x})$, $\alpha_2(\mathbf{x})$, $\beta_2(\mathbf{x})$, but this dependence is suppressed. The quantities $\mathbf{v}$, θ_2, α_2, β_2, $z^+_{\theta_2}, \ldots, z^-_{\beta_2}$ are Lagrangian multipliers. We shall take advantage of all the conditions that follow from the stationary condition $\delta L = 0$, where

$$\delta L = \frac{\partial L}{\partial \mathbf{u}}\,\delta\mathbf{u} + \frac{\partial L}{\partial \theta_2}\,\delta\theta_2 + \frac{\partial L}{\partial \alpha_2}\,\delta\alpha_2 + \frac{\partial L}{\partial \beta_2}\,\delta\beta_2\,. \tag{87}$$

The condition

$$\frac{\partial L}{\partial \mathbf{u}}\,\delta\mathbf{u} = 0 \tag{88}$$

gives

$$f(\delta\mathbf{u}) - a(\mathbf{v}, \delta\mathbf{u}) = 0. \tag{89}$$

Hence $\mathbf{v}$ solves the equilibrium equation. Since this solution is unique and denoted by $\mathbf{u}$ we conclude that $\mathbf{v} = \mathbf{u}$. The conditions

$$\frac{\partial L}{\partial \theta_2}\,\delta\theta_2 = 0\,, \qquad \frac{\partial L}{\partial \alpha_2}\,\delta\alpha_2 = 0\,, \qquad \frac{\partial L}{\partial \beta_2}\,\delta\beta_2 = 0 \tag{90}$$

imply the point-wise (with respect to $\mathbf{x} \in \Omega$) conditions

$$\begin{aligned}
&\frac{\partial C_{ijkl}}{\partial \theta_2}\,\varepsilon_{ij}(\mathbf{u})\,\varepsilon_{kl}(\mathbf{u}) = \Lambda(1 - \alpha_2 - \beta_2 + \alpha_2\beta_2) + z^+_{\theta_2} - z^-_{\theta_2},\\
&\qquad z^-_{\theta_2} \geq 0\,, \qquad z^+_{\theta_2} \geq 0\,, \qquad z^-_{\theta_2}\theta_2 = 0\,, \qquad z^+_{\theta_2}\,(\theta_2 - 1) = 0,\\
&\frac{\partial C_{ijkl}}{\partial \alpha_2}\,\varepsilon_{ij}(\mathbf{u})\,\varepsilon_{kl}(\mathbf{u}) = \Lambda(1 - \theta_2 - \beta_2 + \theta_2\beta_2) + z^+_{\alpha_2} - z^-_{\alpha_2},\\
&\qquad z^-_{\alpha_2} \geq 0\,, \qquad z^+_{\alpha_2} \geq 0\,, \qquad z^-_{\alpha_2}\alpha_2 = 0\,, \qquad z^+_{\alpha_2}\,(\alpha_2 - 1) = 0,\\
&\frac{\partial C_{ijkl}}{\partial \beta_2}\,\varepsilon_{ij}(\mathbf{u})\,\varepsilon_{kl}(\mathbf{u}) = \Lambda(1 - \theta_2 - \alpha_2 + \theta_2\alpha_2) + z^+_{\beta_2} - z^-_{\beta_2},\\
&\qquad z^-_{\beta_2} \geq 0\,, \qquad z^+_{\beta_2} \geq 0\,, \qquad z^-_{\beta_2}\beta_2 = 0\,, \qquad z^+_{\beta}\,(\beta_2 - 1) = 0.
\end{aligned} \tag{91}$$

For the intermediate values of the volume fractions

$$0 < \theta_2 < 1\,, \qquad 0 < \alpha_2 < 1\,, \qquad 0 < \beta_2 < 1\,, \tag{92}$$

the above conditions can be written as

$$\begin{aligned}
&\frac{\frac{\partial C_{ijkl}}{\partial \theta_2}\,\varepsilon_{ij}(\mathbf{u})\,\varepsilon_{kl}(\mathbf{u})}{\Lambda(1 - \alpha_2 - \beta_2 + \alpha_2\beta_2)} = 1,\\
&\frac{\frac{\partial C_{ijkl}}{\partial \alpha_2}\,\varepsilon_{ij}(\mathbf{u})\,\varepsilon_{kl}(\mathbf{u})}{\Lambda(1 - \theta_2 - \beta_2 + \theta_2\beta_2)} = 1,\\
&\frac{\frac{\partial C_{ijkl}}{\partial \beta_2}\,\varepsilon_{ij}(\mathbf{u})\,\varepsilon_{kl}(\mathbf{u})}{\Lambda(1 - \theta_2 - \alpha_2 + \theta_2\alpha_2)} = 1.
\end{aligned} \tag{93}$$

7. The numerical algorithm

The numerical algorithm is based on the finite element method for solving the equilibrium problem (10)–(12) with effective moduli given by Eq. (77). The optimization procedure is written according to COC scheme described in Sec. 6. All examples are restricted to the case of a parallelepiped shape of Ω. The domain Ω is divided into regular 3D solid 8-node linear brick elements see Fig. 3. The computations have been performed with using C3D8 finite element of the ABAQUS system.

The dimensions of a master element are Mod_x, Mod_y, Mod_z; the dimensions of the prism are: $\mathrm{L}_x = \mathrm{N}_x \cdot \mathrm{Mod}_x$, $\mathrm{L}_y = \mathrm{N}_y \cdot \mathrm{Mod}_y$, $\mathrm{L}_z = \mathrm{N}_z \cdot \mathrm{Mod}_z$, where N_x, N_y, N_z are numbers of the brick elements along subsequent sides of the prism.

The optimization algorithm is divided into 21 steps.

Step 1. Fix the data: N_x, N_y, N_z, Mod_x, Mod_y, Mod_z; the boundary conditions and loads, Young moduli E_α and Poisson ratios ν_α; $\alpha = 1, 2$. We select $E_1 < E_2$ and $-1 < \nu_\alpha < 0.5$ such that $\kappa_1 < \kappa_2$ and $\mu_1 < \mu_2$.

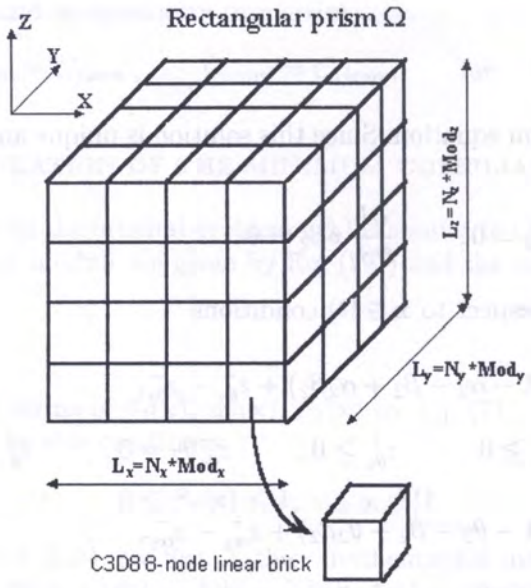

Fig. 3. Division of Ω into regular brick elements

Step 2. Compute the volume $V = \mathrm{L}_x \mathrm{L}_y \mathrm{L}_z$ of the prism Ω and the total number of finite elements N.

Step 3. Let us notice that from the isoperimetric condition (83) and under the assumption of the initial volume fractions $\theta_2 = \theta_2^{(0)}$, $\alpha_2 = \alpha_2^{(0)}$, $\beta_2 = \beta_2^{(0)}$ for $\theta_2^{(0)}$, $\alpha_2^{(0)}$, $\beta_2^{(0)}$ being constant in Ω, we can easily deduce that

$$\left[\theta_2^{(0)} + \alpha_2^{(0)}\left(1 - \theta_2^{(0)}\right) + \beta_2^{(0)}\left(1 - \alpha_2^{(0)}\right)\left(1 - \theta_2^{(0)}\right)\right] V = V_2 \,. \tag{94}$$

Hence

$$\beta_2^{(0)} = \frac{V_2 - V\left[\theta_2^{(0)} + \alpha_2^{(0)}\left(1 - \theta_2^{(0)}\right)\right]}{\left(1 - \alpha_2^{(0)}\right)\left(1 - \theta_2^{(0)}\right) V} \tag{95}$$

provided that $\alpha_2^{(0)} < 1$ and $\theta_2^{(0)} < 1$, and next, from the condition $0 \leq \beta_2^{(0)} \leq 1$, we deduce that

$$V\left[\theta_2^{(0)} + \alpha_2^{(0)}\left(1 - \theta_2^{(0)}\right)\right] = V_l \leq V_2 \leq V. \tag{96}$$

So we see that it is convenient to fix at the beginning of the algorithm the initial volume fractions $0 \leq \theta_2^{(0)} < 1$ and $0 \leq \alpha_2^{(0)} < 1$ (e.g. $\theta_2^{(0)} = 0.5$ and $\alpha_2^{(0)} = 0.5$), next to fix the value of the volume $V_2 = V_l + \chi(V - V_l)$, where $\chi \in [0, 1]$ represents the auxiliary coefficient and compute the initial volume fraction $\beta_2^{(0)}$ from the relation (95).

We initialize the components of the orthogonal matrix $\mathbf{Q} = \mathbf{Q}^{(0)}$ by putting $\mathbf{Q}^{(0)} = \mathbf{I}$, $\mathbf{I}$ being the unit matrix of dimensions 3 by 3.

Step 4. Fix the value of the Lagrange multiplier Λ and material volume tolerance δ needed in numerical calculations: $|V_2 - \text{computed } V_2| \leq \delta$.

Step 5. Fix the non-dimensional parameters: ζ called the move limit and η called a damping factor needed in optimality criteria method (see step 19 below).

Step 6. Initialize the counter of the main loop of the optimization algorithm $k = 0$.

In the next steps we simplify slightly the notation: $\theta \equiv \theta_2$, $\alpha \equiv \alpha_2$, $\beta \equiv \beta_2$, and introduce a new notation for the lists (vectors) of volume fractions in each element $e = 1, 2, \ldots, N$ and in the kth loop

$$\boldsymbol{\theta}^{(k)} = \left[\theta_e^{(k)}\right]_{e=1,\ldots,N}, \qquad \boldsymbol{\alpha}^{(k)} = \left[\alpha_e^{(k)}\right]_{e=1,\ldots,N}, \qquad \boldsymbol{\beta}^{(k)} = \left[\beta_e^{(k)}\right]_{e=1,\ldots,N}.$$

Similarly we introduce the list of rotation tensors

$$\mathbf{Q}^{(k)} = \left\langle \mathbf{Q}_e^{(k)} \right\rangle_{e=1,\ldots N}, \qquad \text{where} \quad \mathbf{Q}_e^{(k)} = \left[Q_{eij}^{(k)}\right]_{\substack{i=1,\ldots,3 \\ j=1,\ldots 3}}.$$

Step 7. For each element e, compute by Eqs. (68)–(70) the effective moduli $C_{ijmn}^{hhh(k)} = C_{ijmn}^{hhh(k)}\left(\theta_e^{(k)}, \alpha_e^{(k)}, \beta_e^{(k)}\right)$ of the orthogonal third-rank laminate.

Step 8. For each element e, create the 6×6 matrix $\hat{\mathbf{C}}_e^{o(k)}$ according to Eq. (79) and the 6×6 matrix

$$\hat{\mathbf{Q}}_e^{(k)} = \left[\hat{Q}_{eab}^{(k)}\right]_{\substack{a=1,\ldots,6 \\ b=1,\ldots,6}}$$

where $\hat{Q}_{eab}^{(k)}$ are determined by Eq. (80), where Q_{ij} should be replaced with $Q_{eij}^{(k)}$, $i, j = 1, 2, 3$.

Step 9. For each element e compute the elasticity matrix $\hat{\mathbf{C}}_e^{(k)}$ according to the formula (78) or

$$\hat{\mathbf{C}}_e^{(k)} = \left(\hat{\mathbf{Q}}_e^{(k)}\right)^{\mathrm{T}} \hat{\mathbf{C}}_e^{o(k)} \hat{\mathbf{Q}}_e^{(k)}. \tag{97}$$

Step 10. In each element e find the components of the elasticity tensor $\mathbf{C}_e^{(k)}$ using the components of the elasticity matrix $\hat{\mathbf{C}}_e^{(k)}$ from the step 9 according to the formula (81), where $\hat{C}_{ab}$ should be replaced by $\hat{C}_{ab}^{(k)}$, $a, b = 1, \ldots, 6$. Other components can be found by the symmetry properties.

Step 11. Write all data to the output file in an appropriate format. This task must be performed automatically (e.g. by the optimization program) because we have at least thousands formally anisotropic finite elements to handle.

Step 12. Run the solver, i.e. a finite element program of the static analysis.

Step 13. Compute the compliance $f^{(k)} = f^{(k)}\left(\mathbf{u}^{(k)}\right)$ of the structure and for each element e initialize the components of the stress tensor $\boldsymbol{\sigma}_e^{(k)} = \left[\sigma_{eij}^{(k)}\right]_{3\times 3}$ and strain tensor $\boldsymbol{\varepsilon}_e^{(k)} = \left[\varepsilon_{eij}^{(k)}\right]_{3\times 3}$ with the results obtained from the solver. Here $\mathbf{u}^{(k)}$ represents the displacement vector of all the nodes of the finite element ensemble.

Step 14. For each element e, find three eigenvectors

$$\mathbf{v}_{e,q}^{(k)} = \begin{bmatrix} \mathrm{v}_{e,q,1}^{(k)} \\ \mathrm{v}_{e,q,2}^{(k)} \\ \mathrm{v}_{e,q,3}^{(k)} \end{bmatrix} \in R^3, \qquad q = 1,2,3,$$

of the matrix $\boldsymbol{\sigma}_e^{(k)}$, i.e. find the solution of the eigenvalue problem $\boldsymbol{\sigma}_e^{(k)}\mathbf{v}_e^{(k)} = \omega_e^{(k)}\mathbf{v}_e^{(k)}$ and create all 6 rotation 3×3 matrices depending on the three eigenvectors $\mathbf{v}_{e,q}^{(k)}$ (the number of permutation of the three element set equals 6):

$$\mathbf{Q}_{e,1}^{(k)} = \begin{bmatrix} \left(\mathbf{v}_{e,1}^{(k)}\right)^{\mathrm{T}} \\ \left(\mathbf{v}_{e,2}^{(k)}\right)^{\mathrm{T}} \\ \left(\mathbf{v}_{e,3}^{(k)}\right)^{\mathrm{T}} \end{bmatrix}, \quad \mathbf{Q}_{e,2}^{(k)} = \begin{bmatrix} \left(\mathbf{v}_{e,1}^{(k)}\right)^{\mathrm{T}} \\ \left(\mathbf{v}_{e,3}^{(k)}\right)^{\mathrm{T}} \\ \left(\mathbf{v}_{e,2}^{(k)}\right)^{\mathrm{T}} \end{bmatrix}, \quad \mathbf{Q}_{e,3}^{(k)} = \begin{bmatrix} \left(\mathbf{v}_{e,2}^{(k)}\right)^{\mathrm{T}} \\ \left(\mathbf{v}_{e,1}^{(k)}\right)^{\mathrm{T}} \\ \left(\mathbf{v}_{e,3}^{(k)}\right)^{\mathrm{T}} \end{bmatrix},$$

$$\mathbf{Q}_{e,4}^{(k)} = \begin{bmatrix} \left(\mathbf{v}_{e,2}^{(k)}\right)^{\mathrm{T}} \\ \left(\mathbf{v}_{e,3}^{(k)}\right)^{\mathrm{T}} \\ \left(\mathbf{v}_{e,1}^{(k)}\right)^{\mathrm{T}} \end{bmatrix}, \quad \mathbf{Q}_{e,5}^{(k)} = \begin{bmatrix} \left(\mathbf{v}_{e,3}^{(k)}\right)^{\mathrm{T}} \\ \left(\mathbf{v}_{e,1}^{(k)}\right)^{\mathrm{T}} \\ \left(\mathbf{v}_{e,2}^{(k)}\right)^{\mathrm{T}} \end{bmatrix}, \quad \mathbf{Q}_{e,6}^{(k)} = \begin{bmatrix} \left(\mathbf{v}_{e,3}^{(k)}\right)^{\mathrm{T}} \\ \left(\mathbf{v}_{e,2}^{(k)}\right)^{\mathrm{T}} \\ \left(\mathbf{v}_{e,1}^{(k)}\right)^{\mathrm{T}} \end{bmatrix}. \tag{98}$$

Step 15. For each element e and for each rotation matrix $\mathbf{Q}_{e,p}^{(k)}$, $p = 1,\ldots,6$, compute the elasticity tensor $\mathbf{C}_{e,p}^{(k)}$, $p = 1,\ldots,6$, according to the rules from the steps 8, 9, 10 using the same matrix $\mathbf{C}_e^{hhh(k)}$ and replacing six times the matrix $\mathbf{Q}_e^{(k)}$ with the matrices $\mathbf{Q}_{e,p}^{(k)}$, $p = 1,\ldots,6$.

Step 16. For each element e, compute six times the elastic energy for matrices $\mathbf{C}_{e,p}^{(k)}$, $p = 1,\ldots,6$ and select rotation matrix $\mathbf{Q}_{e,q}^{(k)}$, $q \in \{1,2,\ldots,6\}$ for which this energy attains the greatest value.

The elastic strain energy $\Xi_e^{(k)} = \frac{1}{2}C_{eijmn}^{(k)}\varepsilon_{eij}^{(k)}\varepsilon_{emn}^{(k)}$ stored in the e-th element for a given elasticity tensor $\mathbf{C}_e^{(k)} = \left[C_{eijmn}^{(k)}\right]$ and the strain tensor $\boldsymbol{\varepsilon}_e^{(k)} = \left[\varepsilon_{eij}^{(k)}\right]$, $i,j,m,n = 1,2,3$, can be computed in a more convenient way by application of the rule $\Xi_e^{(k)} = \frac{1}{2}\hat{\boldsymbol{\sigma}}_e^{(k)} \cdot \hat{\boldsymbol{\varepsilon}}_e^{(k)}$, where the vectors $\hat{\boldsymbol{\sigma}}_e^{(k)} = \left[\hat{\sigma}_{ea}^{(k)}\right]_{a=1,\ldots,6}$, $\hat{\boldsymbol{\varepsilon}}_e^{(k)} = \left[\hat{\varepsilon}_{ea}^{(k)}\right]_{a=1,\ldots,6}$ are defined as in Mehrabadi and Cowin [31] and in Jemioło and Szwed [24],

$$\hat{\boldsymbol{\sigma}}_e^{(k)} = \hat{\mathbf{C}}_e^{(k)}\,\hat{\boldsymbol{\varepsilon}}_e^{(k)}, \tag{99}$$

where

$$\begin{aligned} &\hat{\varepsilon}_{e1}^{(k)} = \varepsilon_{e11}^{(k)}, \qquad \hat{\varepsilon}_{e2}^{(k)} = \varepsilon_{e22}^{(k)}, \qquad \hat{\varepsilon}_{e3}^{(k)} = \varepsilon_{e33}^{(k)}, \\ &\hat{\varepsilon}_{e4}^{(k)} = \sqrt{2}\varepsilon_{e23}^{(k)}, \qquad \hat{\varepsilon}_{e5}^{(k)} = \sqrt{2}\varepsilon_{e13}^{(k)}, \qquad \hat{\varepsilon}_{e6}^{(k)} = \sqrt{2}\varepsilon_{e12}^{(k)}, \end{aligned} \tag{100}$$

and dot $\cdot$ denotes the inner product of the two vectors. So after the step 16 we select an index $q_e^{(k)} = \arg\max_{p=1,\ldots,6}\left\{\frac{1}{2}\hat{\boldsymbol{\sigma}}_{e,p}^{(k)} \cdot \hat{\boldsymbol{\varepsilon}}_e^{(k)}\right\}$ and set $\mathbf{Q}_{e,q}^{(k)} = \mathbf{Q}_{e,q_e^{(k)}}^{(k)}$, where $\hat{\boldsymbol{\sigma}}_{e,p}^{(k)} = \hat{\mathbf{C}}_{e,p}^{(k)}\,\hat{\boldsymbol{\varepsilon}}_e^{(k)}$.

Step 17. For each element e, compute (analytically) all the partial derivatives

$$\frac{\partial C^{hhh(k)}_{e,ijmn}}{\partial\theta}\left(\theta_e^{(k)},\alpha_e^{(k)},\beta_e^{(k)}\right),\qquad \frac{\partial C^{hhh(k)}_{e,ijmn}}{\partial\alpha}\left(\theta_e^{(k)},\alpha_e^{(k)},\beta_e^{(k)}\right),\qquad \frac{\partial C^{hhh(k)}_{e,ijmn}}{\partial\beta}\left(\theta_e^{(k)},\alpha_e^{(k)},\beta_e^{(k)}\right),\quad i,j,m,n=1,2,3$$

and their counterparts rotated by $\mathbf{Q}_e^{(k)}$

$$\frac{\partial C^{(k)}_{e,ijmn}}{\partial\theta}\left(\theta_e^{(k)},\alpha_e^{(k)},\beta_e^{(k)}\right),\qquad \frac{\partial C^{(k)}_{e,ijmn}}{\partial\alpha}\left(\theta_e^{(k)},\alpha_e^{(k)},\beta_e^{(k)}\right),\qquad \frac{\partial C^{(k)}_{e,ijmn}}{\partial\beta}\left(\theta_e^{(k)},\alpha_e^{(k)},\beta_e^{(k)}\right),\quad i,j,m,n=1,2,3$$

according to the rules from the steps 8, 9, 10 and (computed in step 16) the rotation matrix $\mathbf{Q}^{(k)}_{e,q}$.

Step 18. We adjust the Lagrange multiplier Λ appearing in Eq. (86) and strictly linked with the fixed volume condition (83). For initial Lagrange multiplier from step 4 we find simultaneously the new volume fractions $\boldsymbol{\theta}^{k+1}$, $\boldsymbol{\alpha}^{k+1}$, $\boldsymbol{\beta}^{k+1}$ and the new Lagrange multiplier Λ in order to satisfy the active volume constraint (83). The volume of the updated values of volume fractions is a continuous and decreasing function of the multiplier Λ and even strictly decreasing in the intervals, where the bounds on the volume fractions are not active at all points. This allows us to determine uniquely the value of Λ, using e.g. the bisection method, see Bendsøe [6]. In step 19 a very simple algorithm for finding the required value of Λ with given tolerance is presented.

Step 19. Devised in Bendsøe [6] — yet slightly changed in the present paper — a fix-point type updating scheme for the volume fractions in the 2D case is used here for the 3D problem being solved. We start with the Lagrange multiplier Λ fixed in step 4. In each element e, we update $\theta_e^{(k)}$, $\alpha_e^{(k)}$, $\beta_e^{(k)}$ according the scheme

$$\gamma_e^{(k+1)}=\begin{cases}\max\left\{(1-\zeta)\gamma_e^{(k)},0\right\} & \text{if (i)}\\ \gamma_e^{(k)}\left[\Gamma(\gamma_e^{(k)})\right]^{\eta} & \text{if (ii)}\\ \min\left\{(1+\zeta)\gamma_e^{(k)},1\right\} & \text{if (iii)}\end{cases}\tag{101}$$

$$\begin{aligned}&\text{(i)}\quad \gamma_e^{(k)}\left[\Gamma(\gamma_e^{(k)})\right]^{\eta}\le\max\left\{(1-\zeta)\gamma_e^{(k)},0\right\},\\ &\text{(ii)}\quad \max\left\{(1-\zeta)\gamma_e^{(k)},0\right\}\le\gamma_e^{(k)}\left[\Gamma(\gamma_e^{(k)})\right]^{\eta}\le\min\left\{(1+\zeta)\gamma_e^{(k)},1\right\},\\ &\text{(iii)}\quad \min\left\{(1+\zeta)\gamma_e^{(k)},1\right\}\le\gamma_e^{(k)}\left[\Gamma(\gamma_e^{(k)})\right]^{\eta},\end{aligned}\tag{102}$$

where

$$\gamma_e^{(k)}\quad\text{represents}\quad\theta_e^{(k)}\quad\text{or}\quad\alpha_e^{(k)}\quad\text{or}\quad\beta_e^{(k)}\tag{103}$$

and

$$\Gamma\left(\theta_e^{(k)}\right)=\frac{\dfrac{\partial C^{(k)}_{e,ijmn}}{\partial\theta}\left(\theta_e^{(k)},\alpha_e^{(k)},\beta_e^{(k)}\right)\varepsilon^{(k)}_{e,ij}\,\varepsilon^{(k)}_{e,mn}}{\Lambda\left(1-\alpha_e^{(k)}-\beta_e^{(k)}+\alpha_e^{(k)}\beta_e^{(k)}\right)}$$

or

$$\Gamma\left(\alpha_e^{(k)}\right) = \frac{\frac{\partial C_{e,ijmn}^{(k)}}{\partial \alpha}\left(\theta_e^{(k)}, \alpha_e^{(k)}, \beta_e^{(k)}\right) \varepsilon_{e,ij}^{(k)} \varepsilon_{e,mn}^{(k)}}{\Lambda\left(1 - \theta_e^{(k)} - \beta_e^{(k)} + \theta_e^{(k)}\beta_e^{(k)}\right)} \tag{104}$$

or

$$\Gamma\left(\beta_e^{(k)}\right) = \frac{\frac{\partial C_{e,ijmn}^{(k)}}{\partial \beta}\left(\theta_e^{(k)}, \alpha_e^{(k)}, \beta_e^{(k)}\right) \varepsilon_{e,ij}^{(k)} \varepsilon_{e,mn}^{(k)}}{\Lambda\left(1 - \theta_e^{(k)} - \alpha_e^{(k)} + \theta_e^{(k)}\alpha_e^{(k)}\right)} . \tag{105}$$

Let us define (in programming meaning) a function $h : R \mapsto R$, $h = h(\lambda)$ as follows: first for a given value of Lagrange multiplier λ and volume fractions $\boldsymbol{\theta}^{(k)}$, $\boldsymbol{\alpha}^{(k)}$, $\boldsymbol{\beta}^{(k)}$ find new volume fractions $\boldsymbol{\theta}^{(k+1)}$, $\boldsymbol{\alpha}^{(k+1)}$, $\boldsymbol{\beta}^{(k+1)}$ according to the above rules. Next compute the new volume of the subdomain occupied by the material "2",

$$V_2^{(k+1)} = \sum_{e=1}^{N}\left[\theta_e^{(k+1)} + \alpha_e^{(k+1)}\left(1 - \theta_e^{(k+1)}\right) + \beta_e^{(k+1)}\left(1 - \alpha_e^{(k+1)}\right)\left(1 - \theta_e^{(k+1)}\right)\right] V_e,$$

where $V_e = \mathrm{Mod}_x \cdot \mathrm{Mod}_y \cdot \mathrm{Mod}_z = \mathrm{const}$ denotes the volume of the e-th finite element. The computed volume of the domain occupied by the material "2" depends on λ so the difference $V_2^{(k+1)}(\lambda) - V_2$, as a returned value, defines the function $h(\lambda)$. The best value returned by the function $h(\lambda)$ is 0. Numerically, we break computations when the returned value is less or equal to a very small number δ.

It is convenient to look for the best value of Λ together with finding the new volume fractions $\boldsymbol{\theta}^{(k+1)}(\Lambda)$, $\boldsymbol{\alpha}^{(k+1)}(\Lambda)$, $\boldsymbol{\beta}^{(k+1)}(\Lambda)$ according to the scheme outlined in Fig. 4.

Step 20. Set $\forall e \in \{1, \ldots, N\}$ $\quad \mathbf{Q}_e^{(k+1)} = \mathbf{Q}_{e,q}^{(k)}$

Step 21. Set $k = k + 1$ and go to step 7. □

The stop condition of the algorithm can depend on individual preferences.

The condition of stabilization of the values of the compliance as read off from the file in step 13 of the algorithm seems the most reasonable. However, in the examples reported in the present paper the number of the main loops of the algorithm was a priori fixed.

The short outline of the scheme of the implemented program is the following. The optimization program Opty (written in C++ language) reads the output text file written by the Solver — the program of the static analysis, (compliance, stress/strain components) and writes the input text file read by the Solver system (geometry, mesh generation, boundary conditions, loads, updated material properties, etc.) after each main loop of the topology optimization process. In the main program Bond (written in C language), the process-based technique is applied for the concurrent invoking of these two programs. Generally, the programs Opty and Solver are called in Bond alternately — similarly as in producer/consumer relationship. The problem of the synchronization and communication between these programs is solved by using the fork(), wait() and execlp(...) functions, accessible in the environment of the Unix operation system. The program of the visualization of the presented optimal layouts is written in Basic language and was compiled in the environment of the MicroStation graphical system.

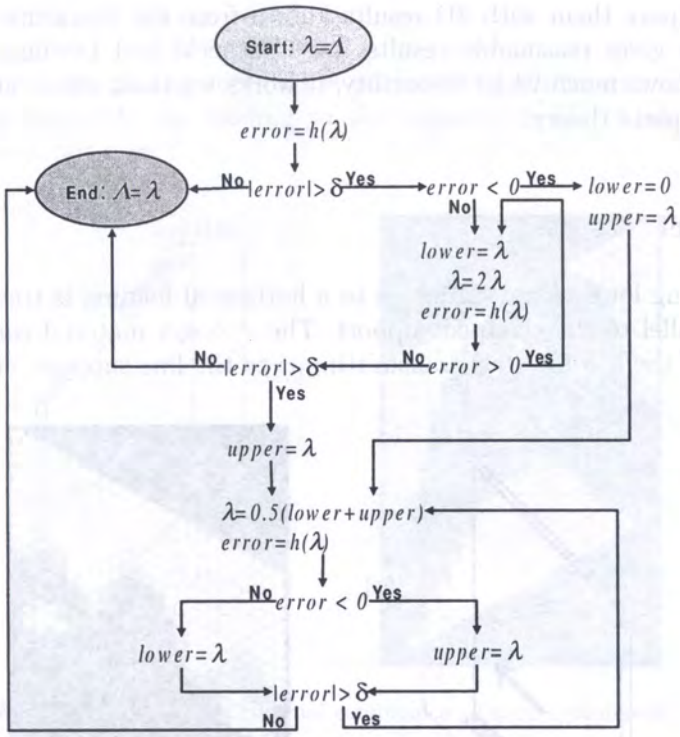

Fig. 4. Algorithm of finding the Lagrange multiplier Λ

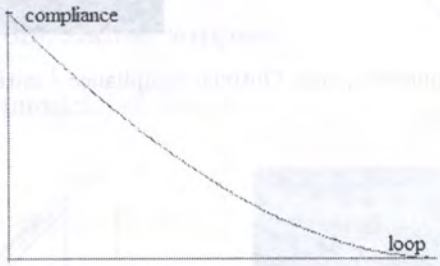

Fig. 5. Typical compliance decay in the main loop of the COC algorithm

In all examples presented below, the Young moduli and Poisson ratios of both the materials are assumed as: $E_1 = 55.0$ [GPa], $E_2 = 210.0$ [GPa], $\nu_1 = 0.25$, $\nu_2 = 0.28$, $V_2 = 78.125\%\ V$. For better visualization of the final results the brick finite elements are replaced by balls inscribed into them. The results presented concern distribution of the m_2 within the feasible domain. This field represents the volume fraction of the stronger material. Its values vary within the interval $[0, 1]$. The case of $m_2 = 0$, shown in white, means that the place is occupied by the weaker material. The opposite case of $m_2 = 1$, shown in black, means that the given place is filled up with the stronger phase. The intermediate values of the m_2 field are shown in a gray scale. All the results shown refer, to dozens iterations ($40 \div 60$ iterations) for less than 3000 finite elements. The typical convergence character of the structure compliance is shown in Fig. 5.

8. Case studies

The examples below concern plates or 3D bodies, all analyzed with using brick elements for 3D elasticity. In the case of plates the optimization could have been performed with using plate elements or within the plate theory. One of the aims of the examples is to consider the results obtained by

3D approach and compare them with 2D results known from the literature. Conclusion is rather positive, 2D approach gives reasonable results, see Czarnecki and Lewiński [12] (2001), yet the approach given here shows much wider versatility, it works for thick plates and for the loading not acceptable within the plate theory.

8.1. Supported panel

A panel supported along lower edge, subjected to a horizontal loading is treated here as 3D plate-like body applied parallel to the clamped support. The stronger material concentrates around the point of application of the loading thus transmitting it to the line support, cf. Fig. 6.

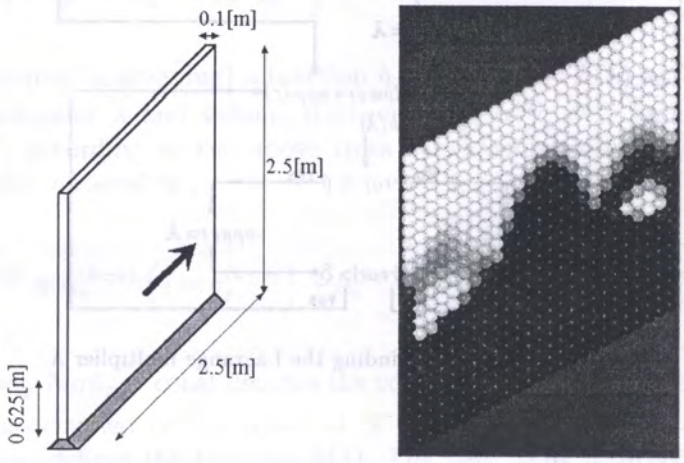

Fig. 6. Clamped supported panel. Optimal compliance / initial compliance = 0.84

8.2. Supported panel

A panel supported along lower edge is now subjected to a horizontal loading at its top edge. The stronger material transmits the loading to the corners, cf. Fig. 7.

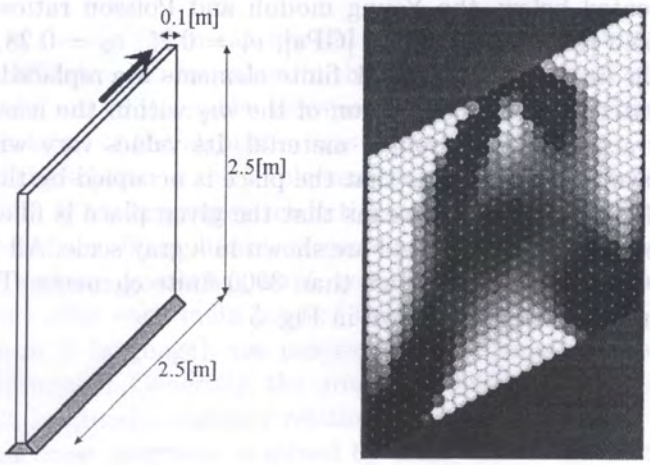

Fig. 7. Clamped supported panel. Optimal compliance / initial compliance = 0.92

8.3. Pin pointed panel

A panel supported at two non-sliding supports is subjected to a horizontal loading at its top edge. The stronger material transmits the loading to the corners, cf. Fig. 8 yet the layout is slightly different than in the previous case.

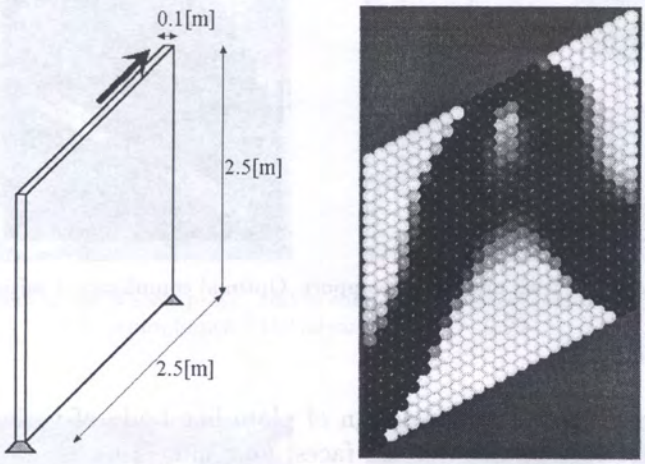

Fig. 8. Pin pointed panel. Optimal compliance / initial compliance = 0.86

8.4. Pin pointed panel with one sliding support

The problem ceases to be antisymmetric, cf. Fig. 9.

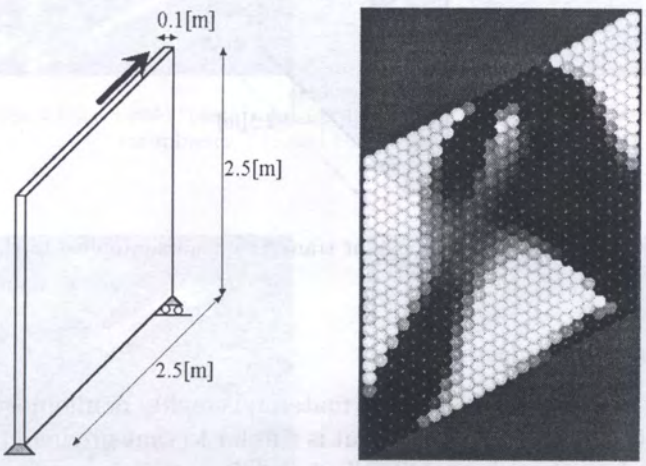

Fig. 9. Pin pointed panel with one sliding support. Optimal compliance / initial compliance = 0.87

8.5. Pin pointed panel with one sliding support, vertically loaded

The layout differs from that predicted within Michell approach for the case of small amount of the stronger material.

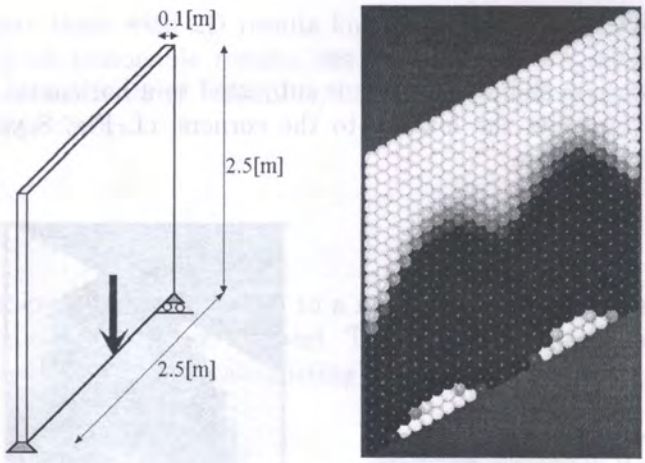

Fig. 10. Pin pointed panel with one sliding support. Optimal compliance / initial compliance = 0.85

8.6. 3D plate-like body

The subject of consideration is optimum design of plate like body of various boundary conditions subjected to a transverse load applied to its faces. Our aim is to assess accuracy of the results obtained previously by the thin plate approach.

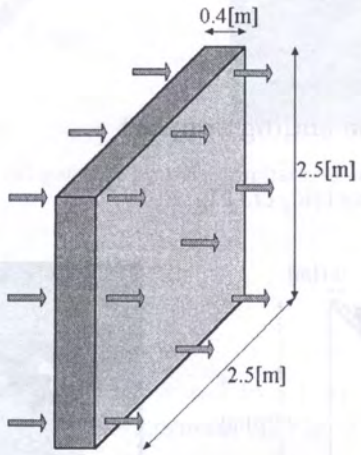

Fig. 11. 3D plate-like body subjected to constant transverse loading applied to the back and front faces

a) Fully clamped plate along all edges

We observe that the distribution of the stronger material is highly nonhomogeneous in the transverse direction. Nevertheless, the overall optimal layout is similar to that predicted by optimizing the plate treated within the thin plate theory, see Olhoff *et al.* [35] and Czarnecki and Lewiński [12]

b) Plate simply supported along all edges

In the case of simple support the stronger concentrates closed to the faces, thus forming a sandwich type plate, cf. Fig. 13.

c) A plate supported at four vertices

The concentrated reactions at the vertices bring about grouping of the stronger material near the corners, see Fig. 14.

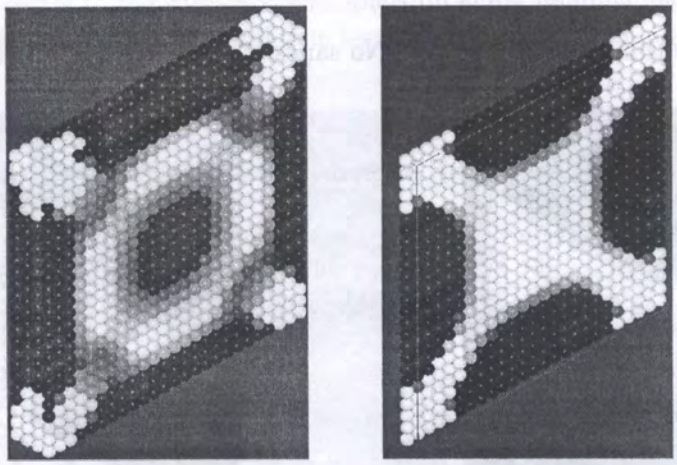

Fig. 12. Isometric view of the whole "plate" and isometric view of the middle vertical section. Optimal compliance / initial compliance = 0.90

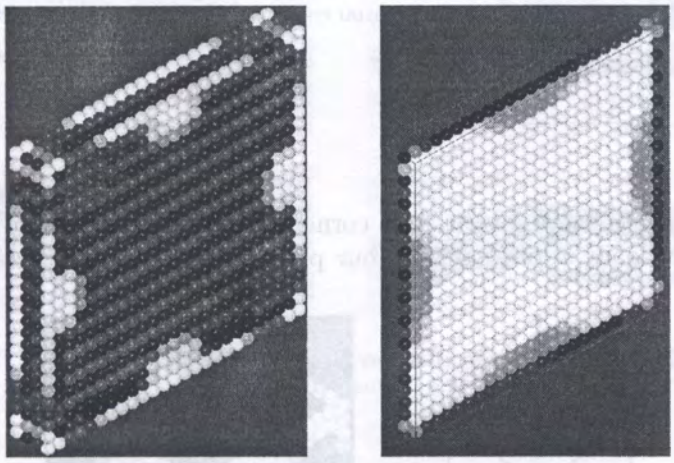

Fig. 13. Isometric view of the whole "plate" and isometric view of the middle vertical section. Optimal compliance / initial compliance = 0.97

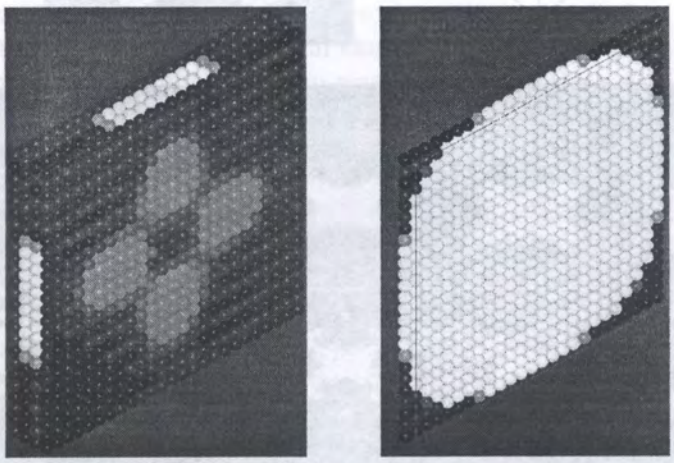

Fig. 14. Isometric view of the whole "plate" and isometric view of the middle vertical section. Optimal compliance / initial compliance = 0.94

d) A thick plate-like body clamped along all edges

The result exceeds the thin plate framework. No sandwich type form is observed, see Fig. 15.

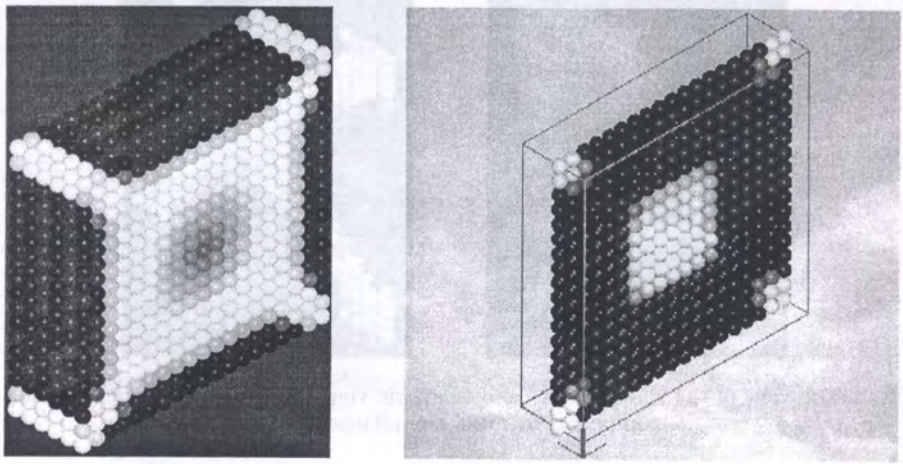

Fig. 15. Isometric view of the whole "plate" and isometric view of the middle vertical section. Optimal compliance / initial compliance = 0.95

8.7. 3D brick

We consider 3D brick, supported at the four corners of the bottom square plane and subjected to concentrated vertical loads applied to the four points of the upper face. The stronger material

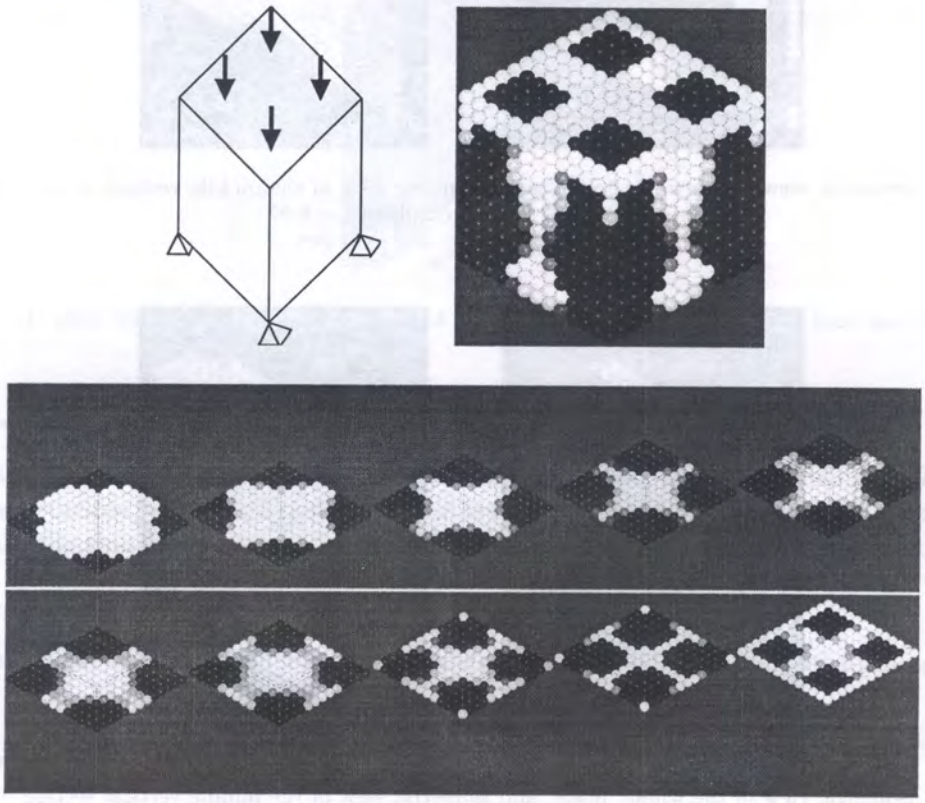

Fig. 16. 3D brick, supported at the four corners. Optimal compliance / initial compliance = 0.81

transmits the forces directly to the supports, which results a chair-like solution. In the case of shape design with smaller amount of the material, the legs of the "chair" are more slender, see Jacobsen *et al.* [23].

8.8. "3D bridge", supported at two edges, loaded vertically along bridge span

The loading is applied at the lower edge surface, which causes concentration of the stronger material along this boundary surface. Thus a lower girder emerges, see Fig. 17. Other numerical results of the bridge problem can be found in Allaire *et al.* [3], Ohmori and Cui [34].

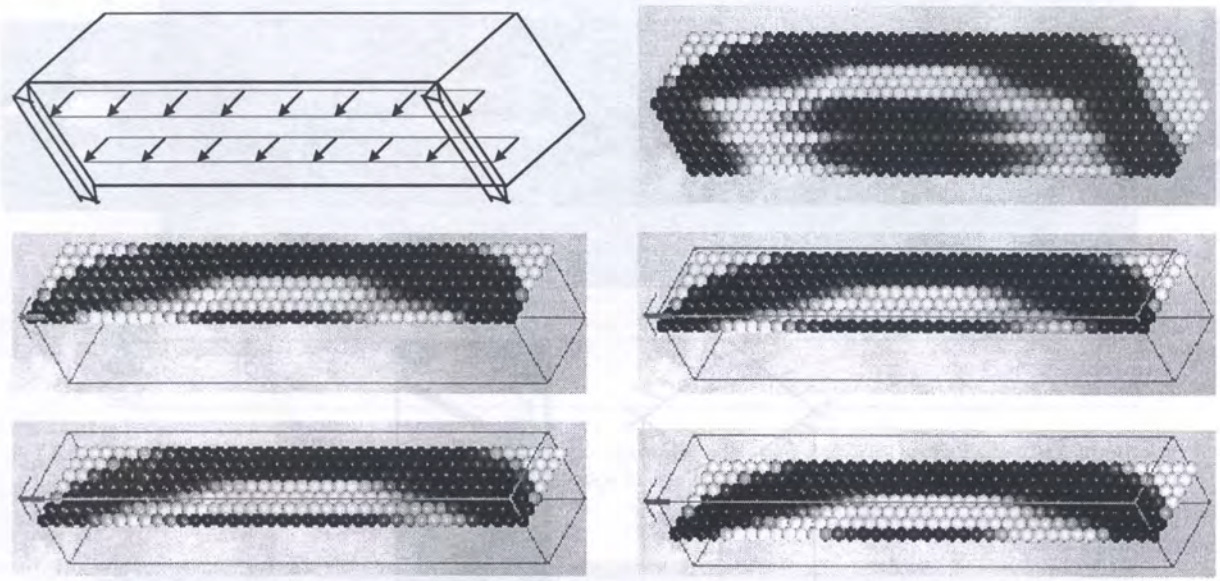

Fig. 17. "3D bridge", supported at two edges, loaded vertically along bridge span. Optimal compliance / initial compliance = 0.91

8.9. Torsion of a 3D brick

We consider torsion of a 3D brick, supported in the middle of the bottom face and subjected to a torque, replaced by a "tangent" horizontal, concentrated forces applied to the four points of the upper face. The torsion causes a specific optimal shape in which the weaker material concentrates around the vertices, see Fig. 18. Similar problem was discussed in Beckers [5].

8.10. The oblong problem

We consider the optimal material distribution associated with transverse torque applied within a 3D prism shown in Fig. 19, called an oblong. The longitudinal slices explain the way the torque is transmitted to the lateral sides, see Fig. 19 and the result published by Jacobsen *et al.* [23].

8.11. A curved shell modelled by 3D finite elements in CAE environment

Alternatively, the user can define the whole 3D structure in graphical environment so the first Solver (ABAQUS in our computations) input file is created automatically by Opty program on the base of the file created in CAE project. The result below was found with using this alternative method.

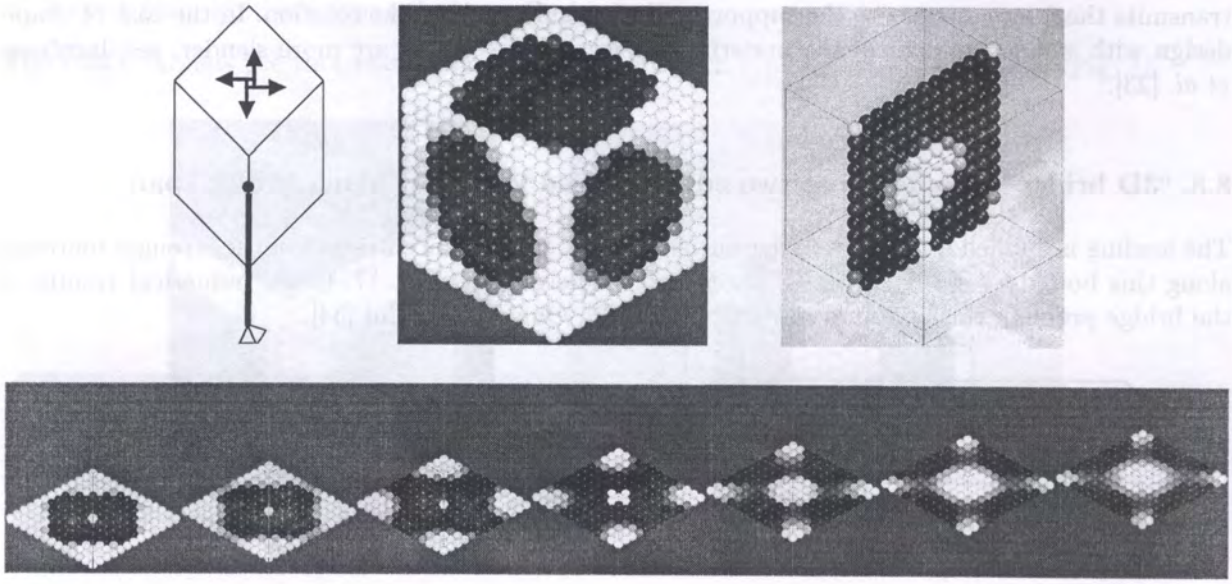

Fig. 18. Torsion of a 3D brick. Optimal compliance / initial compliance = 0.89. Isometric view, vertical section and sequence of horizontal slices through the optimal solution

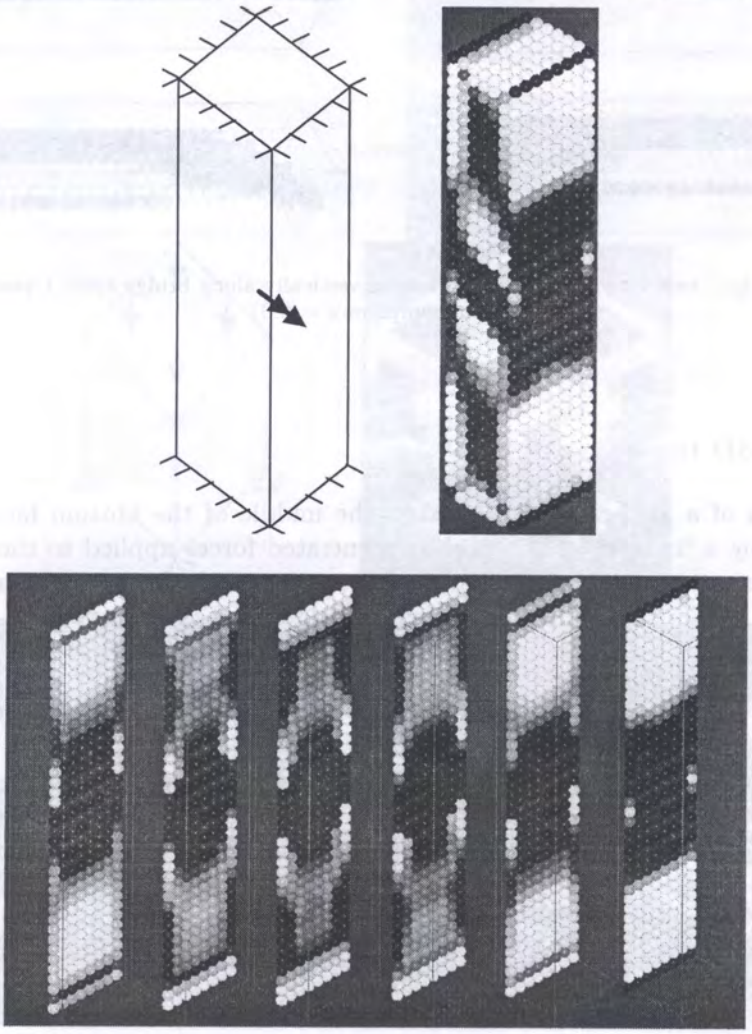

Fig. 19. Optimal compliance / initial compliance = 0.81

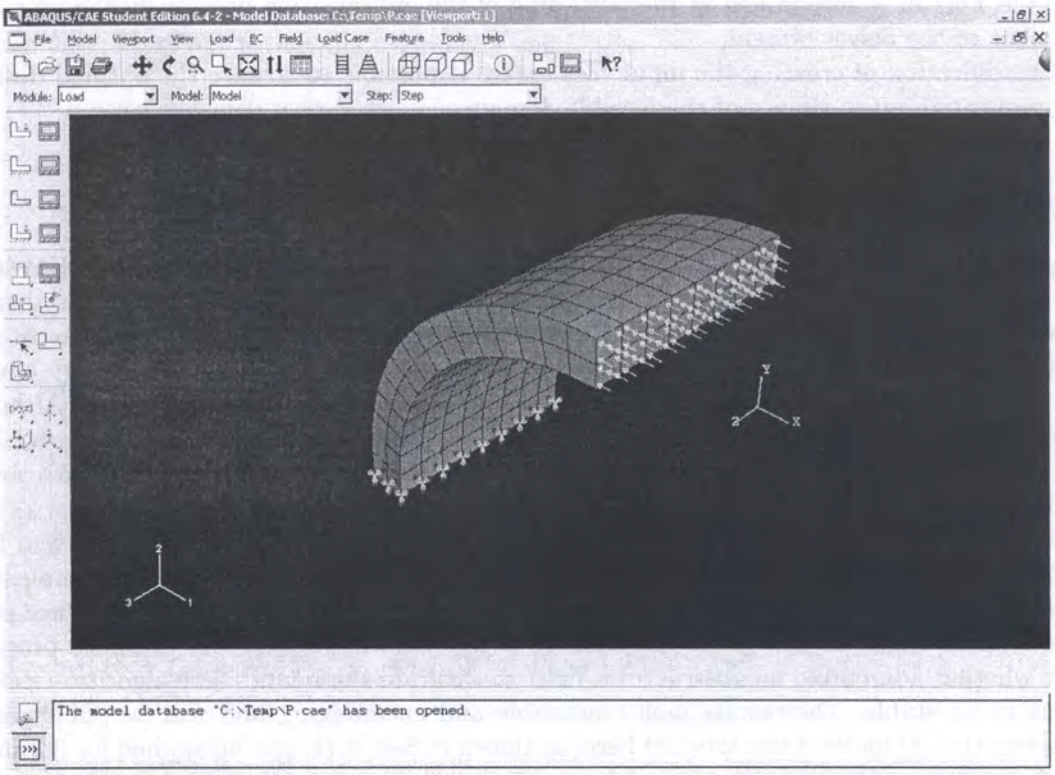

Fig. 20. The view of the support conditions at the clamped edge and uniform pressure loading applied to the parallel edge of the structure

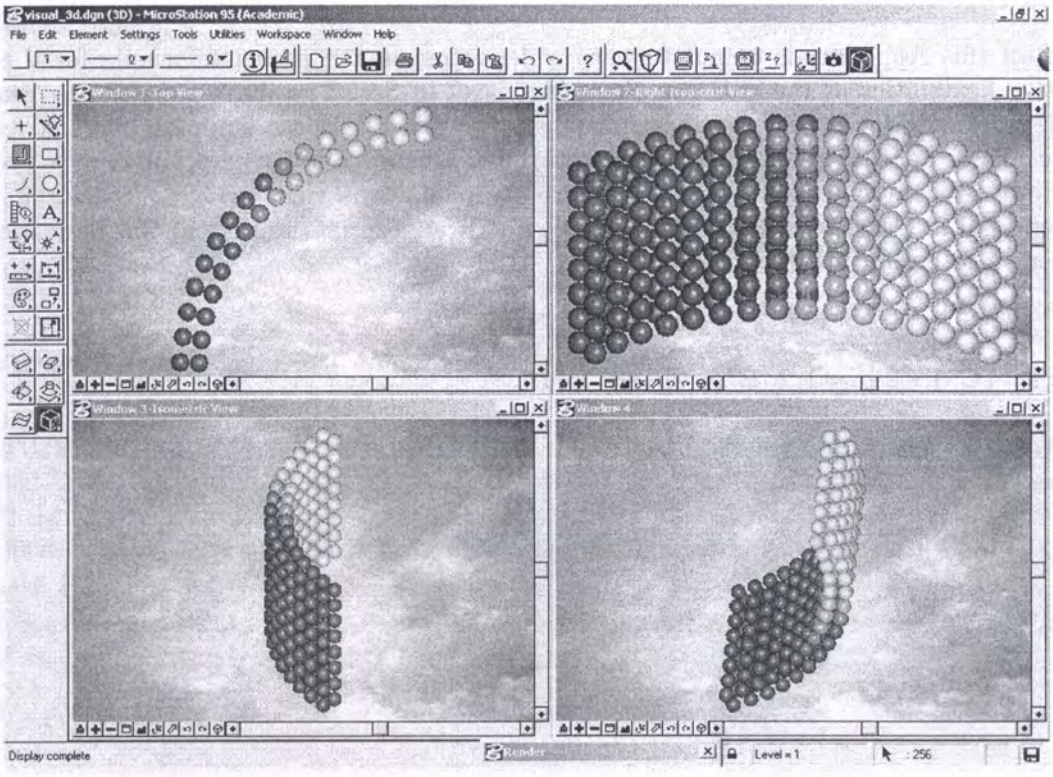

Fig. 21. The optimal layout in various views generated in graphical environment of the MicroStation system, after running of the visualisation program written in MicroStation Basic language

The view in Fig. 20 is determined at the beginning of the optimization process by the user in CAE environment of the Solver system.

This modification of creating the input files makes it possible to achieve the optimal designs for more complicated initial shapes of the feasible domain.

9. Final remarks

The approach proposed is suitable in the case when we make use of given commercial FEM software since it omits sensitivity analyses indispensable while solving the problem by the mathematical programming tools based on gradient methods. Moreover, the approach presented is the most natural for 3D modeling as corresponding to the simplest microstructures saturating the energy bound.

The algorithm presented applies exclusively to the minimum compliance problem. Although in the other optimization problems one should expect that the higher rank laminates will be still helpful, these laminates will for sure possess more complicated micro-geometries, with mutually non-orthogonal stacking directions.

In the case of shells treated within available 2D models a similar optimization problem has not been explicitly solved till now. In the recent papers [15–17] some new estimates of complementary energy have made it possible to arrive at almost-relaxed form of the minimum compliance problem of shallow shells made of one given material. It is not known whether the estimate proposed is sharp or whether admissible microstructures exist to saturate the bound. The algorithm developed turns out to be stable. The results look reasonable and encouraging and will be published soon. Nevertheless the 3D method put forward here, as shown in Sec. 8.11, can be applied for 3D shell-like bodies thus circumventing all the difficulties arising at the interface between the theory of shells and theory of optimal design.

Appendix

The aim of this Appendix is to put forward a derivation of the iterative formula for the tensor of effective flexibilities of the stiff two-phase laminate. In Sec. 3 we have recalled the Francfort-Murat [19] formula for the effective moduli tensor $\mathbf{C}^h$ of a two-phase laminate, with at least one isotropic phase. Specific needs of the theory of the minimum compliance problem of a two-phase elastic body requires an explicit form of this formula for the tensor $\mathbf{c}^h = (\mathbf{C}^h)^{-1}$. Since the formula for $\mathbf{c}^h$ reported in Cherkaev [9] is not explicit we find it appropriate to present this derivation. The main result can be put in the form

$$\theta_1(\mathbf{c}^h - \mathbf{c}^2)^{-1} = (\mathbf{c}^1 - \mathbf{c}^2)^{-1} - \theta_2 \Xi^2, \tag{A1}$$

where $\mathbf{c}^\alpha = (\mathbf{C}^\alpha)^{-1}$, $\alpha = 1, 2$, $\Xi^2 = 2\mu_2 \Psi^2$, and

$$\Psi^2_{pqkl} = -\eta_2 \Pi_{pqkl}(\mathbf{n}) + \Phi_{pqkl}(\mathbf{n}) - I_{pqkl}\,. \tag{A2}$$

Here

$$\Pi_{pqkl}(\mathbf{n}) = (\delta_{pq} - n_p n_q)\,(\delta_{kl} - n_k n_l)\,, \tag{A3}$$

$$\Phi_{pqkl}(\mathbf{n}) = \frac{1}{2}\,(\delta_{qk} n_p n_l + \delta_{ql} n_k n_p + \delta_{pk} n_q n_l + \delta_{pl} n_k n_q) - n_p n_q n_k n_l\,, \tag{A4}$$

$$I_{pqkl} = \frac{1}{2}\,(\delta_{pk}\delta_{ql} + \delta_{qk}\delta_{pl})\,, \tag{A5}$$

and

$$\eta_2 = \frac{\kappa_2 - \frac{2}{3}\mu_2}{\kappa_2 + \frac{4}{3}\mu_2}\,, \qquad \eta_2 = \frac{\nu_2}{1 - \nu_2}\,. \tag{A6}$$

Let us recall the available set of algebraic equations linking the stresses and strains in the strips of the laminate, observed within the periodicity cell

$$\sigma_{ij}^h = \theta_1\sigma_{ij}^1 + \theta_2\sigma_{ij}^2\,, \qquad \theta_1 + \theta_2 = 1, \tag{A7}$$

$$\varepsilon_{ij}^h = \theta_1\varepsilon_{ij}^1 + \theta_2\varepsilon_{ij}^2\,, \qquad \varepsilon_{ij}^h = c_{ijkl}^h\sigma_{kl}^h\,, \qquad \varepsilon_{ij}^1 = c_{ijkl}^1\sigma_{kl}^1\,, \qquad \varepsilon_{ij}^2 = c_{ijkl}^2\sigma_{kl}^2\,, \tag{A8}$$

$$\sigma_{ij}^1 n_j = \sigma_{ij}^2 n_j\,, \qquad \varepsilon_{ij}^2 - \varepsilon_{ij}^1 = p_i n_j + n_i p_j\,. \tag{A9}$$

Let us define the auxiliary quantities

$$\rho_{ij} = (c_{ijkl}^2 - c_{ijkl}^1)\,\sigma_{kl}^1\,, \qquad L_{ij} = \sigma_{ij}^2 - \sigma_{ij}^1\,. \tag{A10}$$

Hence we have

$$\sigma_{ij}^h = \sigma_{ij}^1 + \theta_2 L_{ij}\,, \qquad \sigma_{ij}^h = \theta_1\left[(\mathbf{c}^2 - \mathbf{c}^h)^{-1}\right]_{ijkl}\rho_{kl}\,, \qquad \sigma_{ij}^1 = \left[(\mathbf{c}^2 - \mathbf{c}^1)^{-1}\right]_{ijkl}\rho_{kl}\,. \tag{A11}$$

The above equations lead to the formula:

$$\left\{\theta_1\left[(\mathbf{c}^2 - \mathbf{c}^h)^{-1}\right]_{ijkl} - \left[(\mathbf{c}^2 - \mathbf{c}^1)^{-1}\right]_{ijkl}\right\}\rho_{kl} = \theta_2 L_{ij}\,. \tag{A12}$$

We shall prove that $L_{ij} = 2\mu_2\Psi_{ijkl}^2\rho_{kl}$ with $\mathbf{\Psi}^2$ defined by Eq. (A2).

The relations (A9) and (A10) imply

$$\mathbf{L} = \mathbf{C}^2(\mathbf{n}\otimes\mathbf{p} + \mathbf{p}\otimes\mathbf{n} - \rho)\,. \tag{A13}$$

The condition $(\text{A9})_1$ means that $\mathbf{Ln} = \mathbf{0}$, hence we find the set of equations with unknowns (p_i),

$$2C_{ijkl}^2 n_j n_k p_k = C_{ijkl}^2 n_j \rho_{kl}\,. \tag{A14}$$

This relation implies

$$\mathbf{p}\cdot\mathbf{n} = \frac{1}{2\left(\kappa_2 + \frac{4}{3}\mu_2\right)}\left[2\mu_2 n_l n_k + \left(\kappa_2 - \frac{2}{3}\mu_2\right)\delta_{kl}\right]\rho_{kl}\,. \tag{A15}$$

Taking this result into account in Eq. (A14) one finds $\mathbf{p}$ and

$$(p_i n_j + p_j n_i) = D_{ijkl}\rho_{kl} \tag{A16}$$

where

$$D_{ijkl} = \eta_2 n_i n_j \delta_{kl} + \frac{1}{2}\left(\delta_{jk}n_i n_l + \delta_{jl}n_k n_i + \delta_{ik}n_l n_j + \delta_{il}n_k n_j\right) - 2\,\frac{\kappa_2 + \frac{\mu_2}{3}}{\kappa_2 + \frac{4\mu_2}{3}}\,n_i n_j n_k n_l \tag{A17}$$

and η_2 is given by Eq. (A6). Substitution of Eq. (A16) into (A13) and (A12) gives Eq. (A1) with $\mathbf{\Psi}^2$ defined by Eq. (A2). The passage from Eq. (A12) to (A1) is justified provided that the matrices $(\mathbf{c}^2 - \mathbf{c}^h)$, $(\mathbf{c}^2 - \mathbf{c}^1)$ are invertible.

The formula (A1) is prepared for further lamination. The material of flexibilities c_{ijkl}^h can be mixed with the material No. 2 in a new direction and the process can be continued. Tensor $\mathbf{\Xi}^2$ becomes a new tensor $\mathbf{\Xi}$. In the case of the material No. 1 being a void the formula for $\mathbf{c}^h$ follows from the assumption: $(\mathbf{c}^2 - \mathbf{c}^1)^{-1} \to \mathbf{0}$, hence the formula (A1) reduces to the form

$$\theta_1(\mathbf{c}^h - \mathbf{c}^2)^{-1} = -\theta_2\mathbf{\Xi} \tag{A18}$$

or

$$\mathbf{c}^h = \mathbf{c}^2 - \frac{\theta_1}{\theta_2}\,\mathbf{\Xi}^{-1}\,. \tag{A19}$$

The second lamination in a direction different from $\mathbf{n}$ makes tensor $\boldsymbol{\Xi}$ invertible.

The two-dimensional counterpart of the formula (A1) can be found in Lewiński and Telega [28, Eqs. 3.9.19, 3.9.32]. Here tensor $\boldsymbol{\Xi}^2$ is replaced with $\boldsymbol{\Xi}^2 = 2\mu\boldsymbol{\Psi}^2$, where

$$\Psi^2_{\alpha\beta\lambda\mu} = -\frac{\kappa_2 - \mu_2}{\kappa_2 + \mu_2}\Pi_{\alpha\beta\lambda\mu}(\mathbf{n}) + \Phi_{\alpha\beta\lambda\mu}(\mathbf{n}) - I_{\alpha\beta\lambda\mu} \tag{A20}$$

and Greek indices run over $1, 2$. However, one can easy prove by inspection that

$$\Pi_{\alpha\beta\lambda\mu}(\mathbf{n}) = \tau_\alpha\tau_\beta\tau_\lambda\tau_\mu\,, \qquad \Phi_{\alpha\beta\lambda\mu}(\mathbf{n}) - I_{\alpha\beta\lambda\mu} = -\Pi_{\alpha\beta\lambda\mu}(\mathbf{n}), \tag{A21}$$

where $\boldsymbol{\tau} = (-n_2, n_1)$ is a unit vector tangent to the lamination direction. Substitution of Eq. (A21) into (A20) simplifies the expression for $\boldsymbol{\Xi}^2$ to the form

$$\Xi^2_{\alpha\beta\lambda\mu} = -\frac{4\kappa_2\mu_2}{\kappa_2 + \mu_2}\tau_\alpha\tau_\beta\tau_\lambda\tau_\mu\,. \tag{A22}$$

This simplification has been overlooked in [28]. Thus we see an analogy between the formula (A1) for flexibilities in the plane elasticity problem and the formula (3.8.34) in [28] for stiffnesses of thin Kirchhoff plates.

In the 3D case there is no such simple relation between tensors at the right-hand side of Eq. (A2). In particular, let us note that the relation $\boldsymbol{\Phi} - \mathbf{I} = -\boldsymbol{\Pi}$ does not hold, since

$$\Pi_{1133} = (n_2)^2 + (n_1 n_3)^2, \qquad \Phi_{1133} - I_{1133} = -(n_1 n_3)^2, \tag{A23}$$

which contradicts (A21).

References

[1] *ABAQUS/Standard, User's Manual, Version 6.2*, Vols. I, III. Hibbitt, Karlsson & Sorensen, Inc. 2001.

[2] G. Allaire. *Shape Optimisation by the Homogenisation Method.* Springer , New York 2002.

[3] G. Allaire, E. Bonnetier, G. Francfort, F. Jouve. Shape optimisation by the homogenisation method. *Numerische Mathematik.* **76**: 27–68, 1997.

[4] G. Allaire, R.V. Kohn. Optimal design for minimum weight and compliance in plane stress using extremal microstructures. *European Journal of Mechanics A/Solids.* **12**: 839–878, 1993.

[5] M. Beckers. *Optimization de structures en variable discrètes*, Thèse de doctorat. Faculté des Sciences Appliquées, Université de Liège, 1997.

[6] M.P. Bendsøe. *Optimization of Structural Topology, Shape and Material.* Springer, Berlin, 1995.

[7] M.P. Bendsøe, O. Sigmund. Material interpolation schemes in topology optimization. *Archives of Applied Mechanics*, **69**: 635–654, 1999.

[8] T. Borrvall, J. Petersson. Large-scale topology optimization in 3D using parallel computing. *Computer Methods in Applied Mechanics and Engineering*, **190**: 6201–6229, 2001.

[9] A. Cherkaev. *Variational methods for structural optimization.* Springer, New York 2000.

[10] S. Czarnecki, G. Dzierżanowski, T. Lewiński. Two-phase topology optimization of plates and three-dimensional bodies. *Proc. 5th World Congress of Structural and Multidisciplinary Optimization*, CD-ROM, Lido di Jesolo, Venice, Italy, 19–23 May 2003.

[11] S. Czarnecki, G. Dzierżanowski, T. Lewiński, J.J. Telega. Topology optimization of shells and surface Michell structures. *Proc. 5th World Congress of Structural and Multidisciplinary Optimization*, CD-ROM, Lido di Jesolo, Venice, Italy, 19–23 May 2003.

[12] S. Czarnecki, T. Lewiński. Optimal layouts of a two-phase isotropic material in thin elastic plates. In: Z. Waszczyszyn, J. Pamin, eds., *Proc. 2nd European Conference on Computational Mechanics, ECCM-2001*, CD-ROM, Cracow, 26–29 June 2001.

[13] S. Czarnecki, T. Lewiński. Computational shaping of the least compliant two-phase three-dimensional bodies. In: T. Burczyński, ed., *15th Int. Conference on Computer Methods in Mechanic*, CD-ROM, Gliwice-Wisła, 3–6 June 2003.

[14] A. Díaz, R. Lipton. Optimal material layout for 3D elastic structures. *Structural Optimization*, **13**: 60–64, 1997.

[15] G. Dzierżanowski. Shape design of shallow shells made of isotropic incompressible material. In: W. Pietraszkiewicz, C. Szymczak, eds., *Shell Structures: Theory and Applications. Proc. of the 8th SSTA Conference, Gdańsk-Jurata, October 12–14, 2005*, 101–104. Taylor & Francis / Balkema, London 2005.

[16] G. Dzierżanowski, T. Lewiński. Layout optimization of two isotropic materials in elastic shells. *Journal of Theoretical and Applied Mechanics*, **41**: 459–472, 2003.

[17] G. Dzierżanowski, T. Lewiński. Lower bound on the complementary energy potential in shape optimization problem of shallow shells. In: W. Pietraszkiewicz, C. Szymczak, eds., *Shell Structures: Theory and Applications. Proc. of the 8th SSTA Conference, Gdańsk-Jurata, October 12–14, 2005*, 105–109. Taylor & Francis / Balkema, London 2005.

[18] H.A. Eschenauer, N. Olhoff. Topology optimization of continuum structures: A review. *Applied Mechanics Reviews*, **54**: 331–389, 2001.

[19] G.A. Francfort, F. Murat. Homogenization and optimal bounds in linear elasticity. *Archives of Rational Mechanics and Analysis*, **94**: 307–334, 1986.

[20] G.A. Francfort, F. Murat, L. Tartar. Fourth-order moments of nonnegative measures on S^2 and applications. *Archives of Rational Mechanics and Analysis.* **131**: 305–333, 1995.

[21] L.V. Gibiansky, A.V. Cherkaev. Designing composite plates of extremal rigidity. In: Fiziko-Tekhnichesk. Inst. Im. A.F. Ioffe. AN SSSR, 1984, preprint No 914. Leningrad (in Russian). English translation in: A.V. Cherkaev, R.V. Kohn, eds., *Topics in the Mathematical Modelling of Composite Materials.* Birkhäuser, Boston 1997.

[22] L.V. Gibiansky, A.V. Cherkaev. Microstructures of elastic composites of extremal stiffness and exact estimates of the energy stored in them. In: Fiziko-Tekhnichesk. Inst. Im. A.F. Ioffe. AN SSSR, 1987, preprint No 1115, pp. 52, Leningrad (in Russian). English translation in: A.V. Cherkaev, R.V. Kohn, eds., *Topics in the Mathematical Modelling of Composite Materials.* Birkhäuser, Boston 1997.

[23] J.B. Jacobsen, N. Olhoff, E. Rønholt. Generalized shape optimization of three-dimensional structures using materials with optimum microstructures. *Mechanics of Materials*, **28**: 207–225, 1998.

[24] S. Jemioło, A. Szwed. Application of convex isotropic functions in failure theory for isotropic materials. Yield criteria for metals (in Polish). *Prace Naukowe Politechniki Warszawskiej. Budownictwo*, z. 133, pp. 5–51, 1999.

[25] R.V. Kohn. Recent progress in the mathematical modeling of composite materials. In: G.C. Sih, G.F. Smith, I.H. Marshall, J.J. Su, eds., *Proc. of a Workshop on Composite Material Response: Constitutive Relations and Damage Mechanisms*, 29 pp.. Glasgow, 1987.

[26] L.A. Krog, N. Olhoff. Topology and reinforcement layout optimization of disk, plate and shell structures. In: G.I.N. Rozvany, ed., *Topology Optimization in Structural Mechanics*, pp. 237–322. Springer, Wien–New York, 1997.

[27] R. Kutyłowski. *Optimization of Topology of Material Continuum*, pp. 216 (in Polish). Oficyna Wydawnicza Politechniki Wrocławskiej, Wrocław 2004.

[28] T. Lewiński, J.J. Telega. *Plates, Laminates and Shells. Asymptotic Analysis and Homogenization.* World Scientific. *Series on Advances in Mathematics for Applied Sciences*, vol. 52. Singapore–New Jersey–London–Hong Kong, 2000.

[29] R. Lipton. On a saddle-point theorem with application to structural optimization. *Journal of Optimization Theory and Applications*, **81**: 549–568, 1994.

[30] I. Marczewska, W. Sosnowski, A. Marczewski, T. Bednarek. Topology and sensitivity-based optimization of stiffened plates and shells. *Proc. 5th World Congress of Structural and Multidisciplinary Optimization*, CD-ROM, Lido di Jesolo, Venice, Italy, 19–23 May 2003.

[31] M.M. Mehrabadi, S.C. Cowin. Eigentensors of linear anisotropic elastic materials. *Quarterly Journal of Mechanics and Applied Mathematics*, **43**: 15–41, 1990.

[32] G. Milton. *Theory of Composites.* Cambridge University Press, Cambridge, 2002.

[33] G.W. Milton, A.V. Cherkaev. What elasticity tensors are realizable? *Journal of Engineering Materials and Technology*, **117**: 483–493, 1995.

[34] H. Ohmori, C. Cui. Computational morphogenesis by extended ESO method for 3-dimensional structures. *Proc. of the international IASS symposium on Lightweight Structures in Civil Engineering*, pp. 410–415, Warsaw, Poland, 24–28 June 2002.

[35] N. Olhoff, E. Rønholt, J. Scheel. Topology optimization of three-dimensional structures using optimum microstructures. *Structural Optimization*, **16**: 1–18, 1998.

[36] J. Rychlewski. Unconventional approach to linear elasticity. *Archives of Mechanics*, **47**: 149–171, 1995.

[37] Z. Wasiutyński *et al.* Optimization with respect to the minimum of potential and maximum of stiffness and minimum of flexibility (in Polish). In: A.M. Brandt, ed., *Criteria and Methods of Optimization of Structures*, pp 20–30. Polish Scientific Publ., Warsaw 1977.